

Numerical fluid dynamics for FRG flow equations: Zero-dimensional QFTs as numerical test cases

Part II: Entropy production and irreversibility of RG flows

Adrian Koenigstein,^{1,*} Martin J. Steil,^{2,†} Nicolas Wink,^{2,3,‡} Eduardo Grossi,^{4,§} and Jens Braun^{2,5,6,¶}

¹*Institut für Theoretische Physik, Goethe University,
Max-von-Laue-Straße 1, D-60438 Frankfurt am Main, Germany*

²*Technische Universität Darmstadt, Department of Physics, Institut für Kernphysik, Theoriezentrum,
Schlossgartenstraße 2, D-64289 Darmstadt, Germany*

³*Institut für Theoretische Physik, University Heidelberg,
Philosophenweg 16, D-69120 Heidelberg, Germany*

⁴*Center for Nuclear Theory, Department of Physics and Astronomy,
Stony Brook University, Stony Brook, NY 11794, U.S.A.*

⁵*Helmholtz Research Academy Hesse for FAIR, Campus Darmstadt,
D-64289 Darmstadt, Germany*

⁶*ExtreMe Matter Institute EMMI, GSI,
Planckstraße 1, D-64291 Darmstadt, Germany*

(Dated: August 24, 2021)

We demonstrate that the reformulation of renormalization group (RG) flow equations as non-linear heat equations has severe implications on the understanding of RG flows in general. We demonstrate by explicitly constructing an entropy function for a zero-dimensional \mathbb{Z}_2 -symmetric model that the dissipative character of generic non-linear diffusion equations is also hard-coded in the functional RG equation. This renders RG flows manifestly irreversible, revealing the semi-group property of RG transformations on the level of the flow equation itself. Additionally, we argue that the dissipative character of RG flows, its irreversibility and the entropy production during the RG flow may be linked to the existence of a so-called \mathcal{C}/\mathcal{A} -function. In total, this introduces an asymmetry in the so-called RG time – in complete analogy to the thermodynamic arrow of time – and allows for an interpretation of infrared actions as equilibrium solutions of dissipative RG flows equations. The impossibility of resolving microphysics from macrophysics is evident in this framework.

Furthermore, we directly link the irreversibility and the entropy production in RG flows to an explicit numerical entropy production, which is manifest in diffusive and non-linear partial differential equations (PDEs) and a standard mathematical tool for the analysis of PDEs. Using exactly solvable zero-dimensional \mathbb{Z}_2 -symmetric models, we explicitly compute the (numerical) entropy production related to the total variation non-increasing property of the PDE during RG flows towards the infrared limit.

Finally, we discuss generalizations of our findings and relations to the \mathcal{C}/\mathcal{A} -theorem as well as how our work may help to construct truncations of RG flow equations in the future, including numerically stable schemes for solving the corresponding PDEs.

Keywords: entropy, numerical entropy, total variation diminishing, Functional Renormalization Group, conservation laws, numerical fluid dynamics, irreversibility, \mathbb{Z}_2 model, zero-dimensional QFT, \mathcal{C} -theorem

I. INTRODUCTION

Our modern understanding of Quantum Field Theories (QFTs) and particularly phase transitions is built upon the analysis of renormalization group (RG) trajectories. In fact, RG theory facilitates our understanding by connecting microscopic and macroscopic physics in a continuous manner. This is often visualized at the example of block spin transformations [1, 2] which provides an

intuitive picture of so-called RG flows in position space. A modern, functional approach to RG theory is provided by the Functional Renormalization Group (FRG). It allows for non-perturbative studies of QFTs with applications ranging from biophysics over condensed matter to high-energy physics and quantum gravity, see Ref. [3] for a recent overview.

In Refs. [4–7] it is shown that renormalization group flows can be seen as flows in the literal sense. The RG time $t = -\ln(\frac{k}{\Lambda})$, where k is the RG scale in units of energy and Λ is some ultraviolet (UV) reference scale, can be identified with an abstract time and directions in field

* koenigstein@th.physik.uni-frankfurt.de

† msteil@theorie.ikp.physik.tu-darmstadt.de

‡ wink@thphys.uni-heidelberg.de

§ eduardo.grossi@stonybrook.edu

¶ jens.braun@physik.tu-darmstadt.de

space correspond to spatial directions¹, *cf.* Refs. [14–18] for similar identifications in related flow equations. With this at hand, it becomes appealing to look for further connections between the research fields of (numerical) fluid dynamics and RG theory.

Such a connection is discussed in this paper. To be specific, we shall show that the numerical entropy, which is of utmost importance in the theoretical treatment of partial differential equations (PDEs), see, *e.g.*, the textbooks [19–25], has a very close connection to an entropy in the RG flow and further possible connections to the so-called \mathcal{C} -/ \mathcal{A} -functions for RG theories, *cf.* Refs. [26–40] and Sec. V for more details on \mathcal{C} -/ \mathcal{A} -functions.

One of the most important direct consequences of this is that the same “(thermodynamic) arrow of time” or “thermodynamic time asymmetry” [41] identified by the entropy of a PDE, is also present from an RG perspective.

In nature as well as in the PDEs that describe our physical world, entropy is produced by diffusion (dissipation) as well as discontinuities of all kind. Consequently the evolution of such systems and also their numerical solutions are irreversible and usually only weak solutions are accessible numerically [19–25]. As we will demonstrate in this paper, the total variation non-increasing property and related numerical entropy, used to guarantee the stability of numeric solution schemes, can be promoted to a “physical” entropy function sharing some characteristics with a \mathcal{C} -function and its properties transfer from the PDE to the QFT and vice versa. Therefore, RG flows are also not reversible.² This makes the semi-group character of the RG, see, *e.g.*, Ref. [43], explicit. This semi-group character also becomes manifest in Kadanoffs block-spin picture [1, 2, 44, 45]. The irreversibility of RG flows is not just an abstract concept but presents on a practical level in rather simple truncations of the Functional Renormalization Group (FRG) equation.

These statements may have no severe practical implications for studies of, *e.g.*, QCD and condensed-matter systems, where the RG flow is in general followed from small (UV limit) to large length scales (IR limit). In these cases, the dynamics in the long-range limit is predicted from a given known UV action by integrating out high momentum modes along the “natural” RG-time direction. However, in situations where RG flows are followed from large to small length scales, such as studies of the asymptotic safety scenario in QFTs (see Refs. [27, 46–49], Refs. [50, 51] for a recent review in the context of (quantum) gravity, and Refs. [52, 53] for applications in

condensed-matter physics), the question of irreversibility of RG flows and the associated production of entropy may indeed be very relevant.

Whereas RG flows are indeed reversible for certain classes of truncations (of the underlying effective action), we shall demonstrate in the present work (with the aid of simple models) that it becomes formally impossible to reverse RG flows in cases where no truncations of the effective action are made. Even more, already for often employed truncation schemes (*e.g.*, local potential approximations), we shall see that irreversibility associated with numerical entropy production can already be a manifest feature of RG flows. Of course, irreversibility of RG flows does not imply that it is not possible to construct theories which are valid on all scales. It only implies that the search for such theories may in general be more complicated. In any case, generalizations of the arguments presented in our present work may help to provide a fresh view on these aspects (and/or revive some already existing arguments [14–18, 26, 27]).

As we shall discuss below, fixed points still play an important role within the fluid dynamic interpretation of RG flows. In fact, fixed points can be identified with steady-flow solutions and/or (thermal) equilibrium situations on the level of the rescaled dimensionless flow equations, which have advective and diffusive character.

One major benefit of the connection revealed in this paper is that a measure for the irreversibility of the RG flow is explicitly provided via the identification with numerical entropy and especially total variation [21, 22, 25, 54, 55]. Hence, the construction and analysis of such a measure, at least in certain truncations, might be greatly simplified.³ In future, this might also help to single out adequate truncation schemes for RG flow equations as those truncations, which maintain the irreversible character of the flow of the full untruncated system.

This paper is organized as follows: In Sec. II, we briefly discuss the methodological framework of our present study. This includes both the functional RG approach and its correspondence to fluid dynamics. Moreover, we introduce the zero-dimensional $O(1)$ model which underlies our numerical studies. Numerical entropy and the total variation non-increasing property is then discussed in detail in Sec. III. Explicit computations and a detailed analysis of numerical entropy production in a variety of test cases are presented in Sec. IV. In Sec. V, we then give a discussion of the possibility of a generalization of our present findings with respect to the irreversibility of RG flows, entropy production and the \mathcal{C} -theorem to higher-dimensional theories. Finally, our conclusions and a brief outlook can be found in Sec. VI.

¹ A specific example is the RG flow of (the field-space derivative of) a local potential, which can involve advective and diffusive contributions as well as source/sink terms [4–13].

² Note that similar arguments, which link the dissipative character of RG flow equations to the irreversibility of the RG flow, were already brought up in Refs. [16] and [26] already before or parallel to the development of the functional RG framework pioneered in Ref. [42].

³ We note that observations similar to ours have already been pointed out in the works of Refs. [14–16, 27] for related (partially linearized) flow equations.

II. FUNCTIONAL RG, FLUID DYNAMICS, AND THE ZERO-DIMENSIONAL $O(1)$ MODEL

A. FRG framework

This section is dedicated to a brief summary of the key aspects of the FRG and the zero-dimensional $O(1)$ model within this framework. For a comprehensive discussion, we refer to Part I of our series of publications on numerical fluid dynamics and FRG flow equation [6] as well as to Refs. [4, 5, 7, 8, 13] and upcoming publications [11, 12]. For more general reviews on the FRG method, we refer to Refs. [3, 27, 56–61].

The FRG framework is built on an exact RG equation [42, 62–64], which is a functional partial integro-differential equation for the scale-dependent effective average action $\bar{\Gamma}_t[\Phi]$:

$$\partial_t \bar{\Gamma}_t[\Phi] = \text{STr} \left[\left(\frac{1}{2} \partial_t R_t \right) (\bar{\Gamma}_t^{(2)}[\Phi] + R_t)^{-1} \right]. \quad (1)$$

The equation holds for arbitrary dimensions and arbitrary field content, which is summarized in the “super”-field Φ , *cf.* Refs. [65–68]. Here,

$$t = -\ln \left(\frac{k}{\Lambda} \right) \quad (2)$$

is the RG time (note our sign convention), while k/Λ constitutes the ratio of the RG scale k and the UV cutoff scale Λ . The latter is the scale, where the Exact Renormalization Group (ERG) equation is initialized with the classical action $\bar{\Gamma}_{t=0}[\Phi] = \mathcal{S}[\Phi]$. The “super”-trace stands for a trace in field space, momentum-/position-space, as well as all internal spaces, *e.g.*, color, flavor *etc.* and R_t denotes an monotonically decreasing scale-dependent IR regulator function, see, *e.g.*, Refs. [27, 56, 69–72] for details. Solving the ERG equation (1) by integrating the full set of PDEs that can be generated from the ERG via suitable projections, from $t = 0$ to $t \rightarrow \infty$, thus calculating the full quantum IR effective action $\Gamma[\Phi] \equiv \bar{\Gamma}_{t \rightarrow \infty}[\Phi]$, is equivalent to calculating all 1PI- n -point-correlation (vertex) functions via a partition function/functional integral [56, 60, 73–79]. The ERG equation (1) is the direct mathematical implementation of Wilsons idea of the Renormalization Group [44, 45, 80]: Obtaining the macrophysics from the microphysics via gradually integrating out momentum-shells from the UV to the IR, which corresponds to a coarse-graining process in position space, *e.g.*, Kadanoff’s block-spin transformations [1, 2, 61]. Earlier formulations of the RG in terms of similar flow equations can be found in Refs. [14–17, 80–82].

B. The zero-dimensional $O(1)$ -model

For what concerns this paper, we study one of the probably most simplistic QFTs imaginable within this

framework – a zero-dimensional \mathbb{Z}_2 symmetric model or $O(1)$ model⁴. Still, as the interested reader will experience by studying this and the parallel publications of our series [6, 7], as well as Refs. [83–104], this model (and its extension, the zero-dimensional $O(N)$ (vector) model) is non-trivial and can serve as a minimalistic tool to highlight and test fundamental features of and basic methods for QFTs, not only for pedagogical purposes, but also as real benchmark scenarios.

For the zero-dimensional $O(1)$ model, the most general “truncation” to solve the ERG equation (1) is the local potential approximation

$$\bar{\Gamma}_t[\varphi] = U(t, \varphi), \quad (3)$$

where $U(t, \varphi)$ is simply a function of t and the real scalar (mean) field φ that is called the *scale-dependent effective potential*. Space-time or momentum-space dependences of the field or integrations over the former as well as derivatives of the field do not exist. The entire QFT consists of a scalar ϕ (field), which can assume arbitrary real values and can be thought of as a self-interacting “particle” in a single point. The theory is therefore maximally coupled and ultra-local. The only additional requirement, which we impose on $\langle \phi \rangle = \varphi$ and $U(t, \varphi)$, is that the (mean) field transforms as follows

$$\varphi \mapsto \varphi' = -\varphi \quad (4)$$

under \mathbb{Z}_2 -transformations and that $U(t, \varphi)$ is in turn invariant under these transformations

$$U(t, \varphi) = U(t, -\varphi). \quad (5)$$

The RG flow from $t = 0$ to $t \rightarrow \infty$ is initialized with the classical action (here the classical potential),

$$\bar{\Gamma}_{t=0}(\varphi) = U(t=0, \varphi) = \mathcal{S}(\varphi) = U(\varphi), \quad (6)$$

which also represents an ordinary function of φ with \mathbb{Z}_2 -symmetry. Still, in order to render the corresponding partition function as well as the expectation values (9) convergent, $U(\varphi)$ has to be bounded from below and, for $|\varphi| \rightarrow \infty$, it has to grow at least with φ^2 . Nevertheless, there is no need to claim smoothness or analyticity for $U(\varphi)$, as discussed in detail in part I and III of this series of publications [6, 7] and Sec. IV of this work.

The corresponding ERG equation (1) simplifies dras-

⁴ Although being technically imprecise, we mainly refer to the model as the $O(1)$ model, thus the special case $N = 1$ of an $O(N)$ symmetry, where the symmetry is only realized in terms of discrete transformations.

tically for the zero-dimensional $O(1)$ model,⁵

$$\partial_t U(t, \sigma) = \frac{\frac{1}{2} \partial_t r(t)}{r(t) + \partial_\sigma^2 U(t, \sigma)} = \text{Diagram} \quad (7)$$


However, it retains its fundamental one-loop structure and all its characteristic properties as a non-linear parabolic PDE and initial value problem in one “temporal” $t \in [0, \infty)$ and one “spatial” $\sigma \in (-\infty, \infty)$ direction. Furthermore, it remains an exact equation without any truncation.

A major difference to higher-dimensional $O(1)$ models (e.g., when using the LPA-optimized regulator [69, 70]) is the absence of an additional t -dependent factor on the *r.h.s.* of the equations, cf. Refs. [42, 64, 105], which, however, does not conceptually spoil any of our further reasoning. For what follows, we always use a zero-dimensional version of the monotonically decreasing exponential regulator

$$r(t) = \Lambda e^{-t}. \quad (8)$$

Here, the UV cutoff must be chosen sufficiently large, cf. Refs. [6, 106, 107]. A peculiar feature of the zero-dimensional version of the ERG equation (1) is that an integration to $t \rightarrow \infty$ is indeed possible (which can be seen via reparametrization of the RG time and there is no need for a numerical IR cutoff [6, 91]). Nevertheless, we will use non-vanishing IR cutoffs for our numerical calculations in Sec. IV, to be as close as possible to higher dimensional scenarios.

Having performed the t -integration down to the IR limit, we can extract the vertex functions $\Gamma^{(2n)}$ at the physical point⁶ $\langle \phi \rangle = \varphi = \sigma = 0$ by taking (numerical) derivatives of $U(t=0, \sigma)$ *w.r.t.* σ . These vertex functions are in direct relation to the expectation values, see Refs. [6, 91],

$$\langle \phi^{2n} \rangle = \frac{\int_{-\infty}^{\infty} d\phi \phi^{2n} e^{-S(\phi)}}{\int_{-\infty}^{\infty} d\phi e^{-S(\phi)}}, \quad n \in \mathbb{N}_0, \quad (9)$$

which can be calculated numerically up to machine precision (or sometimes even be evaluated analytically). (Here, ϕ denotes the “fluctuating quantum field”.) This fact makes zero-dimensional QFTs an interesting test ground because numerical FRG calculations can be compared against easily attainable exact results from (numerical) integration of Eq. (9), cf. Refs. [83–104].

C. Fluid-dynamic reformulation of the RG flows

In this section, we briefly summarize the main findings of our parallel and upcoming publications [6, 7, 11, 12] and Refs. [4, 5] on the reformulation of the RG flow equation in terms of a fluid-dynamical conservation law.

Taking a derivative *w.r.t.* σ of the flow equation (7), we obtain a scalar one-dimensional (here parabolic) conservation law,

$$\partial_t u(t, x) = \frac{d}{dx} \left(\left[\frac{1}{2} \partial_t r(t) \right] \frac{1}{r(t) + \partial_x u(t, x)} \right), \quad (10)$$

where $\sigma = x$ is identified with a spatial dimension and $u(t, x) \equiv \partial_x U(t, x)$ is the conserved quantity. In fact, Eq. (10) is a non-linear diffusion/heat equation,^{7,8} which can actually be generalized to arbitrary dimension. This conservative formulation and interpretation in terms of (numerical) fluid dynamics has tremendous consequences and benefits for understanding and solving the RG flow equation:

1. Conservative formulations of RG flow equations provide direct access to the highly developed toolbox of numerical fluid dynamics.
2. An interpretation of the RG flow equations as flow equations in the narrow sense of the word makes the dynamics during the flow intuitively understandable. Advective contributions (pions in the $O(N)$ -scenario) transport the conserved quantity $u(t, x)$ along the field space direction $\sigma = x$ (bulk motion) and can cause non-analyticities like shocks and rarefaction waves in field space [4, 5, 112], as is well known for non-linear hyperbolic conservation laws [19–25, 113, 114]. The non-linear diffusive contribution (the radial sigma mode) smears out cusps and jumps in $u(t, x)$ and corresponds to undirected movement of $u(t, x)$ depending on the local “concentration differences”, the gradient $\partial_x u(t, x)$, via a highly non-linear diffusion coefficient. On the level of the LPA approximation, also fermionic contributions to the flow can be easily understood in this framework in terms of source/sink terms, see ,e.g. Ref. [12].

The reformulation of the flow equation (7) as a diffusion equation (10) has direct implications for the goal of the

⁵ Note that we evaluated φ on a “background-field configuration” σ , which is actually not needed for the zero-dimensional $O(1)$ model because the field φ is already space-time-independent. Still, we adopt the conventions used in Ref. [6] and higher-dimensional scenarios.

⁶ There is no (spontaneous) symmetry breaking in zero dimensions [6, 90]. This is a consequence of a special version of the Coleman-Mermin-Wagner-Hohenberg theorem [108–110] or on the level of Eq. (9) simply a consequence of the discrete \mathbb{Z}_2 -symmetry.

⁷ In part I of this series of publications [6] we demonstrate that the conservative formulation generalizes to zero-dimensional $O(N)$ models, which turn out to be a non-linear advection-diffusion equations, and can even be generalized to higher dimensional models involving fermions in terms of advection-diffusion-source/sink equations [4–13].

⁸ Note that the similarities between RG flow equations and the heat equation were already observed before, cf. Refs. [15, 27, 82, 98, 111], but did – to the best of our knowledge – never result in a comprehensive picture.

present paper. As outlined in our parallel discussion in Sec. IV of Ref. [6], diffusion is one specific dissipative process. Dissipative processes go hand in hand with entropy production and irreversibility.⁹ We can therefore conclude that the irreversibility of the RG transformations during the RG flow is hard coded in the diffusive character of the ERG equation (1), not only in zero space-time dimensions, but for any dimension and any QFT, *cf.* Refs. [14–16]. Hence, the rise of entropy during the RG flow might therefore be directly linked to \mathcal{C} -/ \mathcal{A} -theorems. This is explained in the next sections in the context of our minimalistic toy model QFT.

III. (NUMERICAL) ENTROPY AND THE TOTAL VARIATION

The first part of this section deals with the explicit construction of a (numerical) entropy for the conservation law (10). This entropy has to be a functional of the conserved quantity $u(t, x)$ and/or its derivatives¹⁰ that is monotonically rising during the RG flow. Monotonicity is explicitly proven for valid initial conditions $U(t = 0, x)$. Since $u(t, x)$ is by definition a function of all couplings of the theory, the (numerical) entropy function might therefore be linked to a zero-dimensional version of \mathcal{C} -/ \mathcal{A} -function. In fact it might have some practical advantages compared to some practical approaches towards \mathcal{C} -/ \mathcal{A} -functions studied in literature, since $u(t, x)$ does not even need to be expandable in explicit couplings at all, but still contains all degrees of freedom.

In the second part of this section, we derive a discrete formulation of this entropy functional and demonstrate that it can be directly related to the *total variation* (TV) of $u(t, x)$ and the total variation diminishing/non-increasing property (TVD/TVNI) of commonly used numeric schemes for conservation laws [19, 54, 55], which is, by we denote it as a “numerical” entropy.

A. Construction of the (numerical) entropy

The construction of our (numerical) entropy function is directly inspired by the construction of entropy/energy functionals for the Bateman-Burgers equation [117, 118] or the heat-equation [119].

Let $y \in \mathbb{R}$ and

$$s : \mathbb{R} \rightarrow \mathbb{R}, \quad y \mapsto s(y), \quad (11)$$

be a continuously twice differentiable convex function on \mathbb{R} , hence

$$s(y) \in C^2(\mathbb{R}), \quad s''(y) \geq 0, \quad (12)$$

for all $y \in \mathbb{R}$. Furthermore, we require that $s(y)$ shall not grow faster than y^2 for $|y| \rightarrow \infty$, which is explained below. Using $s(y)$ we define the functional

$$S[f(x)] \equiv - \int_{-\infty}^{\infty} dx s(f(x)), \quad (13)$$

to which we shall refer as *entropy functional*. In general, the bounds of integration are chosen according to the domain of our problem at hand. Next, we prove that, choosing $f(x) = \partial_x u(t, x)$, Eq. (13) indeed plays the role of an (numerical) entropy for the partial differential equation (10). Hence, it measures similarly to \mathcal{C} -/ \mathcal{A} -functions for the RG flows the degrees of freedom and irreversibility. To this end, we explicitly demonstrate that $S[\partial_x u(t, x)]$ is a monotonically increasing during the RG flow, thus being a monotonic function on $t \in [0, \infty)$:

$$\frac{d}{dt} S[\partial_x u(t, x)] \geq 0. \quad (14)$$

The only further ingredient, which is needed for the proof is the spatial derivative of the flow-equation (10):

$$\begin{aligned} \partial_t [\partial_x u(t, x)] &= \\ &= - \frac{d}{dx} \left(\left[\frac{1}{2} \partial_t r(t) \right] \frac{\partial_x^2 u(t, x)}{[r(t) + \partial_x u(t, x)]^2} \right). \end{aligned} \quad (15)$$

Taking spatial derivatives of $u(t, \sigma)$ should be allowed at any $t \in (0, \infty)$ because of the smoothening character of the diffusion – at least in zero space-time dimensions.¹¹ Only for $t = 0$ the initial condition may violate smoothness, see part I of this series of publications [6] for a detailed discussion of this subtle issue. Below, we normalize the entropy and subtract the entropy of the initial condition $S[\partial_x u(t = 0, x)]$, such that that this should not spoil any of our subsequent arguments.

Let us now evaluate Eq. (14):

⁹ This argument also generalizes to the $O(N)$ model involving advection and the large- N limit [115]. The corresponding flow equation in the limit $N \rightarrow \infty$ is a purely hyperbolic advection equation. Interacting and arising non-analyticities like shocks and rarefaction waves in non-linear advection equations are sources of entropy and as such lead so irreversible flows, *cf.* Refs. [4, 5, 7, 112, 116] for examples of non-analytical dynamics in RG flows.

¹⁰ The purely diffusive character of Eq. (10) is expected to smoothen u during the RG flow which renders $u(t, x)$ differentiable (but not necessarily analytic) at least for $0 < t < \infty$. This does not need to be the case for hyperbolic conservation laws where taking derivatives of $u(t, x)$ has to be handled with great care, *e.g.*, around shocks.

$$\begin{aligned}
& \frac{d}{dt} S[\partial_x u(t, x)] = \\
&= - \frac{d}{dt} \int_{-\infty}^{\infty} dx s(\partial_x u(t, x)) = \\
&= - \int_{-\infty}^{\infty} dx (\partial_t [\partial_x u(t, x)]) s'(\partial_x u(t, x)) = \\
&= \int_{-\infty}^{\infty} dx \left[\frac{d}{dx} \left(\left[\frac{1}{2} \partial_t r(t) \right] \frac{\partial_x^2 u(t, x)}{[r(t) + \partial_x u(t, x)]^2} \right) \right] s'(\partial_x u(t, x)) = \\
&= \int_{-\infty}^{\infty} dx \left[-\frac{1}{2} \partial_t r(t) \right] \frac{[\partial_x^2 u(t, x)]^2}{[r(t) + \partial_x u(t, x)]^2} s''(\partial_x u(t, x)) + \left[\frac{1}{2} \partial_t r(t) \right] \frac{\partial_x^2 u(t, x)}{[r(t) + \partial_x u(t, x)]^2} s'(\partial_x u(t, x)) \Big]_{-\infty}^{\infty}
\end{aligned} \tag{16}$$

Next, we analyze both terms in the last line separately.

1. We note that all factors in the integrand of the first term are greater or equal to zero: For the regulator insertion, we have

$$-\frac{1}{2} \partial_t r(t) \geq 0, \tag{17}$$

because $r(t)$ is a monotonically decreasing function. The numerator and the denominator are obviously positive. In fact, for the denominator of the fraction

$$r(t) > \partial_x u(t, x), \tag{18}$$

for all t anyhow, as long as the initial condition $u(t=0, x)$ and the UV cutoff Λ are chosen accordingly, *cf.* Ref. [6]. Finally,

$$s''(\partial_x u(t, x)) \geq 0, \tag{19}$$

holds by construction according to Eq. (12).

In total, we find that the integrand of the first term is always greater or equal to zero, which directly transfers to the integral itself.

2. For the second term, we first use that, for large $|x|$, the potential $U(t, x)$ and all its derivatives do not change during the RG flow, see also part I of this series of publications [6]. Furthermore, we use that $s(y)$ maximally grows like y^2 for $|y| \rightarrow \infty$ by definition. This implies that its derivative $s'(y)$

increases asymptotically as y at most. Additionally, we use that $U(t, x)$ is at least proportional to x^2 for $|x| \rightarrow \infty$ in order to have well-defined expectation values (9). Consequently, we have to distinguish two scenarios. If $U(t, x) \sim x^2$ for large $|x|$, the second term vanishes identically, due to the third spatial derivative of $U(t, x)$, namely $\partial_x^2 u(t, x)$, in the numerator. Otherwise, if $U(t, x)$ grows faster than x^2 for large $|x|$, the denominator $[r(t) + \partial_x u(t, x)]^2$ will always grow faster than the product $[\partial_x^2 u(t, x)] s'(\partial_x u(t, x))$ for $|x| \rightarrow \infty$. We conclude that the second term always vanishes, provided that the initial conditions come with the assumed large- $|x|$ -asymptotic behavior.

In total, we have shown the statement of Eq. (14), which promotes S to an entropy (functional) of our system that can only increase.

For what follows, we choose the twice differentiable convex function $s(y) = y^2$. This implies

$$S[\partial_x u(t, x)] = - \int_{-\infty}^{\infty} dx [\partial_x u(t, x)]^2. \tag{20}$$

However, this brings up the following problem: For practical purposes $S[\partial_x u(t, x)]$ formally diverges at any time t because $\partial_x u(t, x)$ is at least constant for $|x| \rightarrow \infty$. This problem can be cured, by subtracting the entropy $S[\partial_x u(t=0, x)]$ of the initial condition. Since $u(t, x)$ does not change for large $|x|$ during the entire RG flow, the infinite but constant contributions cancel and we can observe the relative rise in entropy. This should be a valid approach, since we are only interested in these relative changes anyhow. We therefore define and consider the normalized entropy

$$\mathcal{C}[\partial_x u(t, x)] = S[\partial_x u(t, x)] - S[\partial_x u(t=0, x)], \tag{21}$$

which is finite. The alphabetic character “ \mathcal{C} ” is chosen because this function quantifies irreversibility similarly to \mathcal{C} -/ \mathcal{A} -functions. We are aware of the fact that

¹¹ The generalization of this argument to higher-dimensional $O(N)$ -type models might be delicate, because the non-linear diffusion can also cause non-analyticities in potentials in the IR if these end up in the symmetry broken phase. Here it might be unavoidable to base and repeat the entire discussion using a rigorous weak/integral formulation of the PDEs under consideration.

a real \mathcal{C} -/ \mathcal{A} -function should be based on the dimensionless rescaled flow equation. This issue is discussed in Sub.Sec. V A.

B. Discrete formulation and relation to the total variation non-increasing property

In this subsection we discuss a discretized version of Eq. (21), which is suited for practical computations. In the following and *w.l.o.g.* we consider a finite volume (FV) discretization [21, 22, 25, 54] of $u(t, x)$ in x with n volume cells of constant width Δx , centered at x_i , $i \in \{0, 1, \dots, n-1\}$, see our parallel discussion in Sec. IV of Ref. [6] for details. The RG flow is described by the temporal evolution of the n volume averages $\bar{u}_i(t)$, which are formally defined as the spatial averages of $u(t, x)$ over $[x_{i-\frac{1}{2}}, x_{i+\frac{1}{2}}]$, where $x_{i\pm\frac{1}{2}} \equiv x_i \pm \frac{\Delta x}{2}$. For the purpose of calculating $\mathcal{C}[\partial_x u(t, x)]$, we reconstruct the first derivatives from the set of volume averages $\{\bar{u}_i(t)\}$ by a first order finite difference (FD) forward stencil,

$$\partial_x u(t, x_i) = \frac{\bar{u}_{i+1}(t) - \bar{u}_i(t)}{\Delta x} + \mathcal{O}(\Delta x). \quad (22)$$

For the scope of this work this has proven sufficient since the purely diffusive character of the PDE smoothens $u(t, x)$.¹²

We use a grid with the first volume cell of the computational domain centered at zero, $x_0 = 0$, and the last centered at a finite x_{\max} , hence $x_{n-1} = x_{\max}$. x_{\max} is chosen large enough, such that $u(t, x_{\max}) = u(t = 0, x_{\max})$ holds to a sufficient level for all t , compare our discussion in Ref. [6] as well as Refs. [4, 120–122]. This enables a computation of $\mathcal{C}[\partial_x u(t, x)]$ considering only $x \in [-x_{\max}, +x_{\max}]$ since the difference $S[\partial_x u(t, x)] - S[\partial_x u(t = 0, x)]$ practically vanishes for $|x| \geq x_{\max}$. We therefore study the following quantity:

$$\mathcal{C}[\partial_x u(t, x)] = -2 \int_0^{x_{\max}} dx [\partial_x u(t, x)]^2 + \quad (23)$$

¹² However, for non-smooth/non-differentiable initial conditions at $t = 0$, such as Eqs. (27) and (30) of our numeric examples, a naive finite difference stencil is of course generically ill-conditioned at the discontinuities. As a direct consequence, the absolute value of $S[\partial_x u(t = 0, x)]$ strongly depends on the explicit discretization points and the “capturing of the discontinuity” in the respective volume cells. For $t \rightarrow \infty$ (as a direct consequence of the Coleman-Mermin-Wagner-Hohenberg theorem [108–110]), $u(t, x)$ is smooth and the finite difference approximation is well-behaved as long as Δx is not too small. We conclude that the absolute values of our entropy function (21) will strongly depend on Δx for non-differentiable initial conditions in the IR because we use $S[\partial_x u(t = 0, x)]$ as normalization, while the qualitative behavior (monotonic rise) is independent of the discretization, which is also true for the discrete total variation (26). For the smooth initial conditions (28) and (29), we observed little dependence of the absolute values of the $\mathcal{C}[\partial_x u(t, x)]$ on Δx , as expected. Similar discussions will arise for $\mathcal{O}(N)$ -type models in higher-spacetime dimensions, when their RG flows end in the symmetry broken phase with a non-analytic IR-potential.

$$+ 2 \int_0^{x_{\max}} dx [\partial_x u(t = 0, x)]^2,$$

leveraging the \mathbb{Z}_2 -symmetry of the problem at hand. Inserting Eq. (22) and performing the integrals over the constant segments in the volume cells leads to our semi-discrete formulation

$$\mathcal{C}[\{\bar{u}_i(t)\}] = -\frac{2}{\Delta x} \left(\sum_{i=0}^{n-1} \frac{[\bar{u}_{i+1}(t) - \bar{u}_i(t)]^2}{(1 + \delta_{i,0} + \delta_{i,n-1})} - \sum_{i=0}^{n-1} \frac{[\bar{u}_{i+1}(0) - \bar{u}_i(0)]^2}{(1 + \delta_{i,0} + \delta_{i,n-1})} \right), \quad (24)$$

where the factor $(1 + \delta_{i,0} + \delta_{i,n-1})$ takes into account the fact that we only integrate over the right half of the first and the left half of the last volume cell.

Practical computations of solutions to the PDE (10) on the compact interval $x \in [0, x_{\max}]$ require carefully chosen boundary conditions [6, 7] to be consistent with solutions of the pure initial value problem posed by Eq. (10) on the interval $x \in (-\infty, +\infty)$ [121, 123]. In the present finite volume setup we implement boundary conditions with “ghost cells” at x_{-2} , x_{-1} , x_n and x_{n+1} , where the corresponding cell averages are chosen due to the \mathbb{Z}_2 -anti-symmetry of $u(t, x)$ in cases of $\bar{u}_{-2}(t)$ and $\bar{u}_{-1}(t)$ and by means of linear extrapolation in the cases of $\bar{u}_n(t)$ and $\bar{u}_{n+1}(t)$, see Sub.Sec. IV D of part I of this series of publications [6] for details. For the computation of $\mathcal{C}[\{\bar{u}_i(t)\}]$ we require only the ghost-cell average $\bar{u}_n(t) = 2\bar{u}_{n-1}(t) - \bar{u}_{n-2}(t)$ as well as the cell averages at x_i for $i \in \{0, 1, \dots, n-1\}$.

The entropy functional (20) introduced in Sub.Sec. III A is closely related to the total variation [55] – which is simply the arc length – of the solution $u(t, x)$,

$$\text{TV}[\partial_x u(t, x)] \equiv \int_0^{x_{\max}} dx |\partial_x u(t, x)|, \quad (25)$$

on the (computational) interval $[0, x_{\max}]$. The TV qualitatively differs only by a global sign from the entropy functional S , where the sign used for the TV is compatible with the mathematical convention for (numerical) entropy. The use of the absolute value $|\partial_x u(t, x)|$ in Eq. (25) instead of the square $[\partial_x u(t, x)]^2$ used for S presents only as quantitative difference, which is not of any practical relevance in this work.

On a FV grid, a typical discretized version of Eq. (25) is given by, *cf.* Refs. [21, 22, 25, 55],

$$\text{TV}[\{\bar{u}_i(t)\}] \equiv \sum_{i=0}^{n-1} |\bar{u}_{i+1}(t) - \bar{u}_i(t)|, \quad (26)$$

where a first order forward FD stencil is used to discretize the first derivative. The differences $\mathcal{C}[\{\bar{u}_i(t^m)\}] - \mathcal{C}[\{\bar{u}_i(t^{m+1})\}]$ and $\text{TV}[\{\bar{u}_i(t^{m+1})\}] - \text{TV}[\{\bar{u}_i(t^m)\}]$ on a discrete trajectory $\bar{u}_i(t)$ of an admissible solution

at different times separated by one time step Δt , where $t^{m+1} = t^m + \Delta t$, are both greater or equal to zero for all t^m . Thus total variation – arc length – is non-increasing¹³ and the corresponding entropy in the sign convention of this paper is non-decreasing – monotonically increasing.

(Weak) solutions of broad classes of hyperbolic and parabolic conservation laws are total variation non-increasing during time evolution when considered on a finite interval, see, *e.g.*, Refs. [21, 24, 55] and especially Ref. [124]. The flow Eq. (10) under consideration in this paper is a non-linear, parabolic pure diffusion equation and the construction of the normalized entropy functional \mathcal{C} of Eq. (21) can be adapted to prove directly that solutions of the flow Eq. (10) are TVNI. The notion of numerical entropy (and TV as a possible candidate for it) is very important in the study, construction and numerical computation of physical weak solutions of conservative equations, see, *e.g.*, the textbooks [19–25] for further details.

IV. NUMERICAL ENTROPY PRODUCTION IN ZERO-DIMENSIONAL MODELS

In this section we present explicit numerical results for the RG flows of the (numerical) entropy function (21) for some selected zero-dimensional $O(1)$ models (different UV initial conditions). As examples, we choose the test cases which are introduced and discussed in great detail in Sec. V of part I of this series of publications [6]. All information on the explicit numerical treatment is presented in Sec. IV of part I of this series of publications [6], where the Kurganov-Tadmor (KT) central scheme [54] is discussed and applied to RG flow equations. The numerical parameters for the RG flows of this paper are stated in the figures and their respective captions. An elaborated discussion on the choice and tests of numerical and model parameters can also be found in Chap. V of part I of this series of publications [6]. For the sake of completeness and as proof of reliability of our numerical scheme and the choice of our numerical parameters, we nevertheless provide a comparison in Tab. I between numerical results for the 1PI-two-point-function $\Gamma^{(2)}$ calculated via the solution of the flow equation (10) with the KT-scheme and “exact” results calculated via expectation values (9) from the partition function.

Note that all plots of the entropy in this section are based on a direct implementation of Eq. (24).

A. Test case I: Non-analytic initial condition

As our first test case, we choose a UV potential associated with a broken \mathbb{Z}_2 symmetry. Moreover, it shall come with infinitely many degenerate minima as well as non-analytic points at $|\sigma| = 2$ and $|\sigma| = 3$,

$$U(\sigma) = \begin{cases} -\frac{1}{2}\sigma^2, & \text{if } |\sigma| \leq 2, \\ -2, & \text{if } 2 < |\sigma| \leq 3, \\ +\frac{1}{2}(\sigma^2 - 13), & \text{if } 3 < |\sigma|, \end{cases} \quad (27)$$

see Fig. 4 of Ref. [6] and also top panel of Fig. 1 for visualizations. This UV potential amounts to a piecewise linear discontinuous initial condition $u(t=0, x)$ for the RG flow equations (10). The corresponding RG flow of $u(t, x)$ is presented in Fig. 1. The diffusive character of the σ -mode is clearly visible from the fact that it smoothens the discontinuities at $x = 2$ and $x = 3$, without any directed propagation (advection) of the conserved quantity $u(t, x)$. As discussed in Refs. [6, 90], the system has to restore the \mathbb{Z}_2 symmetry in the ground state as dictated by the Coleman-Mermin-Wagner-Hohenberg theorem [108–110]. In particular, the potential has to become convex [79, 126]. This can be directly observed in the plot of the RG flow and read off from Tab. I – the two-point function is positive at $\sigma = 0$.

In Fig. 2 we present the RG flow of the (discretized numerical) entropy function for our first test case. As expected from our discussion in Sec. III, the entropy grows monotonically. It increases by two orders of magnitude starting at zero in the UV until it reaches (again) a plateau in the IR. We find that the entropy grows most when the regulator (8) reaches the model scales. Loosely speaking, this is where most of the dynamics

TABLE I. The table lists the “exact” results for $\Gamma^{(2)}$ of the $O(1)$ model (second column) for the various UV initial potentials of our test cases (first column), which are calculated by a brute force high-precision one-dimensional numerical integration of the expectation values (9) using *NIntegrate* in *Mathematica* [125] with a *PrecisionGoal* and *AccuracyGoal* of 10. Here, we shall present the first ten digits. The last column lists the relative errors of the numerical solution of the RG flow equation with diffusion obtained with the second order accurate KT-central scheme [54] using the parameters listed in the corresponding Figs. 1, 3, 4, 7 and 9, see also Ref. [6] for a detailed discussion of such errors.

UV potential	$\Gamma^{(2)}$	$ \Gamma_{\text{FRG}}^{(2)}/\Gamma^{(2)} - 1 $
(27)	0.1768130358	$6.0 \cdot 10^{-6}$
(28) (neg. mass)	0.1995098930	$1.1 \cdot 10^{-5}$
(28) (pos. mass)	1.3324252475	$1.4 \cdot 10^{-5}$
(29)	0.1740508127	$2.5 \cdot 10^{-5}$
(30)	0.2046977422	$5.8 \cdot 10^{-6}$

¹³ In literature total variation diminishing (TVD) is often used as a less precise synonym for total variation non-increasing (TVNI), *cf.* Sec. 9.2.2 of Ref. [25].

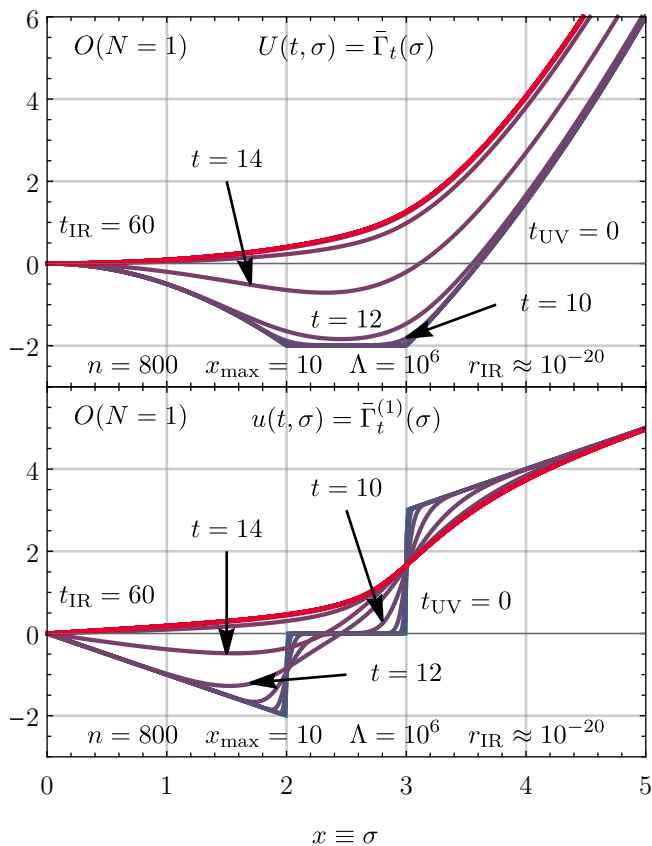


FIG. 1. RG flow of the effective potential $U(t, \sigma)$ (upper panel) and its derivative $u(t, \sigma) = \partial_\sigma U(t, \sigma)$ (lower panel) for the zero-dimensional $O(N = 1)$ -model with initial condition Eq. (27) evaluated at $t = 0, 2, 4, \dots, 60$ (integer values for t were only chosen for convenience and readability). The blue curve corresponds to the UV while the red curve to the IR. We used the exponential regulator Eq. (8) with UV cutoff $\Lambda = 10^6$. For convenience only, the plot does not show the region $x = 5$ to $x = 10$ because the tiny differences between $u(t, \sigma)$ and $u(t_{UV}, \sigma)$ are not visible in this region and vanish for large $x = \sigma$ anyhow. The lower panel is identical to Fig. 8 (upper panel) of Ref. [6].

takes place, see Fig. 1 (approximately between $t \approx 4$ and $t \approx 16$). This is the RG time frame in which the diffusion smears out the discontinuities. From a fluid and thermodynamic perspective and directly on the level of the PDE, the whole process is intuitively understandable: Diffusion goes hand in hand with strong dissipation and a loss of information about the initial state of the system – the UV, *cf.* Ref. [16, 26]. This is directly comparable to heat conduction, where the information about the initial temperature distribution gets lost during the flow towards “thermal” equilibrium [21, 41, 119]. In the RG framework, this translates to integrating out degrees of freedom from the UV to the IR and a growth in the number of coupling constants in $U(t, \sigma)$, which is directly related to the growth of entropy. The entropy plateau in the IR is identified with the interacting IR regime and an

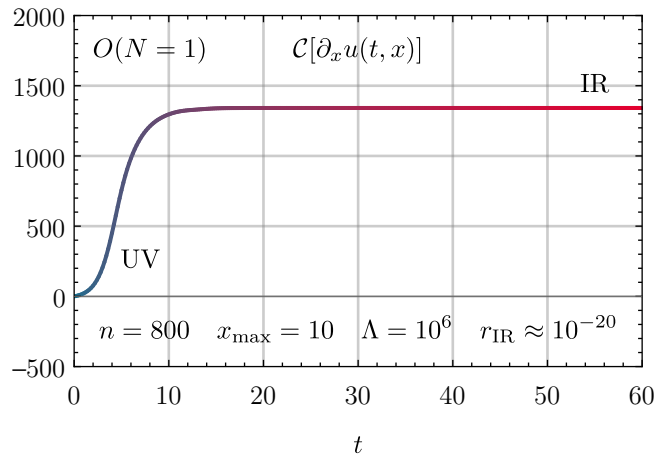


FIG. 2. The plot shows the monotonic growth of the (numerical) entropy/the \mathcal{C} -function $\mathcal{C}[\partial_x u(t, x)]$ during the RG flow of the test case (27) and corresponds to Fig. 1.

“thermal” equilibrium on the level of the diffusive PDE, whereas a plateau in the UV is associated with a Gaussian UV fixed point [75, 127]. As expected the entropy stops changing at these points. IR solutions therefore correspond either to steady-flow solutions (in advection dominated systems for a large number of “Goldstone” modes [128–130]) or to (thermal) equilibrium solutions (in diffusion dominated $O(1)$ -symmetric systems) in the fluid dynamical picture [6].

Note that $t \in [0, 60]$ corresponds to a integration over 26 orders of magnitude in $r(t)$, starting 6 orders of magnitude above the model scales (which are of order one) and ending up 20 orders of magnitude below the model scales. In part I of this series of publications [6], we discussed that large/low UV/IR cutoffs are needed to ensure cutoff independence of the IR effective action, which is also known as RG consistency [106]. Interestingly, we find that the almost total absence of a plateau in the entropy in the UV of our first case implies that we almost violated RG consistency.¹⁴ For all other test cases this is avoided by choosing larger UV cutoffs Λ , see below.

Before we continue with our next test case, we again note that the absolute value of $\mathcal{C}[\partial_x u(t, x)]$ in the IR in Fig. 2 has no quantitative meaning, due to the ill-conditioned behavior when applied to the discontinuous initial condition (27) of the numerical derivative (22). However, this does not spoil our qualitative arguments at all.

¹⁴ The absence of the zero-entropy plateau can also be seen by closer inspection of Fig. 16 of Ref. [6], where $\Lambda = 10^6$ is barely on the plateau of RG consistent UV scales.

B. Test case II: ϕ^4 -theory

The second test case is the zero-dimensional analogue of higher-dimensional ϕ^4 -models. We consider two UV initial conditions, differing in the sign of the mass-like ϕ^2 -contribution,

$$U(\sigma) = \mp \frac{1}{2} \sigma^2 + \frac{1}{4!} \sigma^4. \quad (28)$$

Hence, depending on the sign, we either start the RG flow with a broken \mathbb{Z}_2 -symmetry in the ground state or with a \mathbb{Z}_2 -symmetric ground state. For a visualization of the initial condition with negative mass term, see Fig. 18 of Ref. [6]¹⁵. This initial condition is chosen because of its relevance in higher dimensions, *e.g.*, for studies of spontaneous symmetry breaking and symmetry restoration (ranging from applications in statistical mechanics and condensed-matter theory to high-energy physics). Additionally, in contrast to our first test case (27), due to the analyticity of Eq. (28), a generic expansion of the potential in polynomials at any σ is possible in the UV at $t = 0$. This property can be used to study the convergence of a common FRG truncation scheme, the Taylor expansion of the effective action. In Sec. V of Ref. [6], we find that only for positive mass-like terms, where the physical point does not move during the RG flow, the FRG Taylor expansion about the IR minimum $\sigma = 0$ exhibits “apparent” convergence by increasing the expansion order. For negative mass terms (also using a fixed expansion point at the IR minimum $\sigma = 0$), we do not find convergence while increasing the expansion order. In Sec. V of Ref. [6], we argue that during the RG flow, while the physical point moves from $\sigma = \pm\sqrt{6}$ to $\sigma = 0$, presumably an excessively large or even infinitely many new couplings are generated in $U(t, \sigma)$. This renders FRG Taylor expansion at a finite order a potentially problematic approximation scheme in such a scenario.

In this subsection, we reinforce our findings about the non-convergence of expansions of the potential during the RG flow by studying the (numerical) entropy production during the RG flows. The RG flows of $u(t, x)$ for both initial conditions are depicted in Fig. 3 (for negative mass term) and in Fig. 4 (for positive mass term).¹⁶

Both RG flows are by visual inspection not really spectacular: For the “negative mass”-case, we find that, according to the Coleman-Mermin-Wagner-Hohenberg theorem [108–110], the diffusion via the σ -mode restores the \mathbb{Z}_2 -symmetry and drives the potential convex during the RG flow before the system equilibrates in the IR. For the

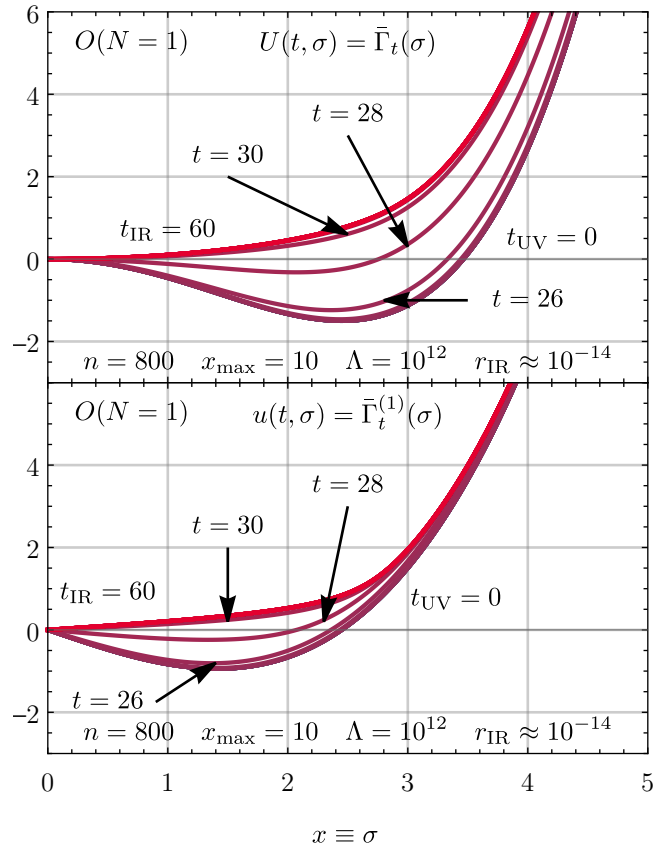


FIG. 3. RG flow of the effective potential $U(t, \sigma)$ (upper panel) and its derivative $u(t, \sigma) = \partial_\sigma U(t, \sigma)$ (lower panel) for the zero-dimensional $O(N = 1)$ -model with initial condition Eq. (28) (with negative mass term) evaluated at $t = 0, 2, 4, \dots, 60$ (integer values for t were only chosen for convenience and readability). The blue/magenta curve corresponds to the UV while the red curve to the IR. We used the exponential regulator Eq. (8) with UV cutoff $\Lambda = 10^{12}$. For convenience only, the plot does not show the region $x = 5$ to $x = 10$ because the tiny differences between $u(t, \sigma)$ and $u(t_{UV}, \sigma)$ are not visible in this region and vanish for large $x = \sigma$ anyhow.

RG flow of the “positive mass”-case we only find minimal changes in the shape of $u(t, x)$ also originating from the non-linear diffusion during the RG flow. Hence, the equilibrated solution in the IR is relatively close to the UV initial potential.

The plots of the corresponding entropies in Fig. 5 (for negative mass term) and Fig. 6 (for positive mass term) are more instructive. In both cases we find a clear monotonic rise of the (numerical) entropy exactly in the RG time period, in which most of the dynamics takes place. Furthermore, we clearly find plateaus in the UV and the IR, which correspond to the trivial UV regime and the non-trivial interacting IR regime. This plateau-like behavior signals RG consistency. In comparison with our first test case (27), where we used exactly the same discretization points (volume cells), the monotonic growth

¹⁵ RG flows for both choices of sign within a low-order FRG Taylor expansion are also provided in, *e.g.*, Refs. [90, 91, 94] for the zero-dimensional $O(N)$ model.

¹⁶ Note that the plot ranges for the “positive mass”-case are different from all other plots of RG flows of $u(t, x)$ in this section. Otherwise, the tiny changes during the RG flow would not be visible at all.

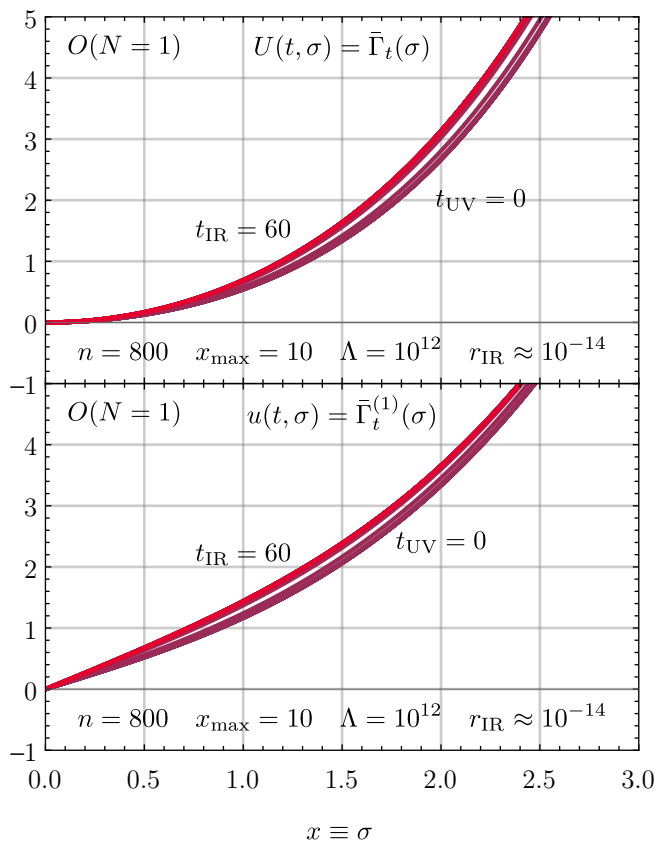


FIG. 4. RG flow of the effective potential $U(t, \sigma)$ (upper panel) and its derivative $u(t, \sigma) = \partial_\sigma U(t, \sigma)$ (lower panel) for the zero-dimensional $O(N = 1)$ -model with initial condition Eq. (28) (with positive mass term) evaluated at $t = 0, 2, 4, \dots, 60$ (integer values for t were only chosen for convenience and readability). The blue/magenta curve corresponds to the UV while the red curve to the IR. We used the exponential regulator Eq. (8) with UV cutoff $\Lambda = 10^{12}$. For convenience only, the plot does not show the region $x = 3$ to $x = 10$ because otherwise the differences between the UV and the IR curves would not be visible at all for the entire domain.

of entropy is less drastic and significantly smaller. This is expected because the jumps in $u(t = 0, x)$ at $x = 2$ and $x = 3$ in the first test case (27) lead to greater changes in the discrete total variation [the arc length in x of $u(t, x)$] than the rather small changes of the profiles of $u(t, x)$ for the ϕ^4 -models, compare Sub.Sec. III B. Also from a fluid dynamic perspective, this is intuitively understandable because the smoothing of huge gradients (rarefaction waves) is a substantial source of entropy and obviously an irreversible process, whereas only a small transport of a fluid is not a source of excessive but rather small entropy production, even-though it is diffusion driven. Still, also for both ϕ^4 -cases the entropy increases during the RG flow, which firstly signals an increasing number of coupling constants generated during the RG flow, and secondly also renders the RG flows irreversible.

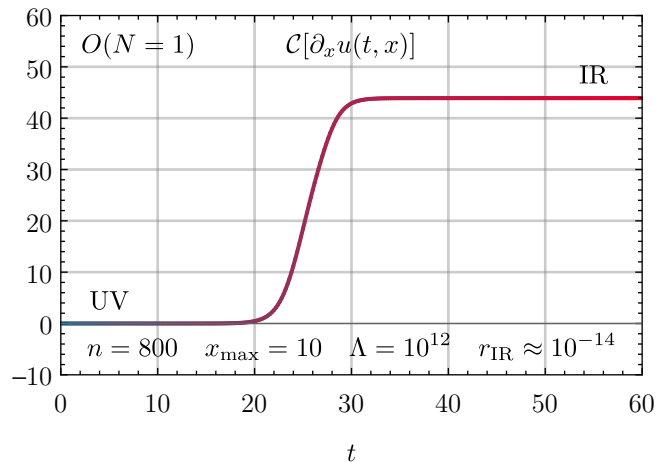


FIG. 5. The plot shows the monotonic growth of the (numerical) entropy/the \mathcal{C} -function $\mathcal{C}[\partial_x u(t, x)]$ during the RG flow of the test case (28) (with negative mass term) and corresponds to Fig. 3.

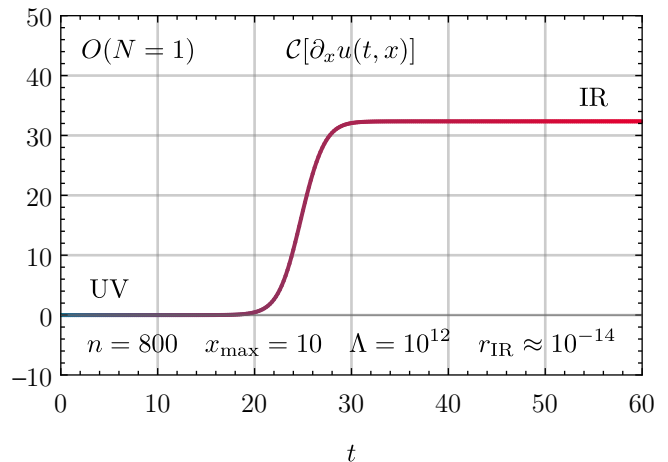


FIG. 6. The plot shows the monotonic growth of the (numerical) entropy/the \mathcal{C} -function $\mathcal{C}[\partial_x u(t, x)]$ during the RG flow of the test case (28) (with positive mass term) and corresponds to Fig. 4.

The second observation has severe consequences: Any RG flow in a FRG Taylor expansion employs a finite set of coupled ODEs for the couplings (vertices). Since the system is finite, it seems to be theoretically possible integrate in either RG time direction. In higher dimensions, one can formally integrate to larger or lower (energy) scales (associated with resolutions in position space), compare with, *e.g.*, the perturbative β -functions of QCD, QED *etc.* [131–134]. However, this is in principle not compatible with the irreversibility of RG flows as shown in our present work (as, *e.g.*, signaled by the rise of entropy) and may only be reliable within small subspaces of the theory space associated with a given theory. In fact, the computation of fundamental couplings

at small scales (high energies) from effective couplings at large scales (low energies) is in general not possible, *cf.* Ref. [2]. We conclude that the increase of entropy, which we also observe during the RG flow of our analytic initial conditions (28) reveals potential limitations of Taylor expansion of effective actions because most likely an extremely large number (or even infinite number) of couplings is generated in the RG flow and would be required to correctly describe the RG flow. ¹⁷¹⁸

In practical computations with the zero-dimensional $O(N)$ model a complete inversion of the RG flow – integrating up from the IR to the UV – is possible only under certain conditions. In Sub.Sub.Sec. V B 2 of part I of this series of publications [6] we performed tests with the ϕ^4 model discussed in this subsection and found that a complete and accurate practical inversion is only possible for the ϕ^4 model with positive mass term when considering a small set of running couplings. Numerical instabilities related to massive oscillations in the higher-order couplings prevent a numerical inversion of the RG flow for larger systems of couplings. In the ϕ^4 model with negative mass term a numerical reconstruction of the non-convex UV potential by integrating up from the convex IR potential seems to be practically impossible with the employed Taylor expansions. While an inversion of the RG flow seems theoretically possible on first sight when considering the finite ODE systems of the FRG Taylor (vertex) expansion the practical/numerical realization is not obvious.

When considering an expansion in vertices, it might be possible that higher-order couplings/vertices are strongly suppressed (especially when considering higher dimensional QFTs), such that an expansion of the ERG equation (1) in vertices is applicable and meaningful in practice, see, *e.g.*, Refs. [107, 135–137]. This should go hand

in hand with only a small growth of an entropy for the exact RG flow. Exactly this seems to be the case for our “positive mass”-case (28), which shows almost no dynamics at all and yields the smallest increase in entropy of all our test cases. A reason, why here a rather small number of couplings might be sufficient to describe the entire RG flow is that the potential is convex during the entire flow and has a single unique non-moving minimum. Hence, the UV regime of this model and the IR regime do not differ much and, as long as the quartic coupling is extremely small, also perturbation theory [92] leads to results which are consistent with the exact values for the lowest 1PI- n -point-correlation (vertex) functions [91].

C. Test case III: ϕ^6 -potential

The third test case describes a potential that is analytic with a \mathbb{Z}_2 -symmetric ground state in the UV. However, the potential exhibits two non-trivial local minima and behaves asymptotically $\propto \phi^6$,

$$U(\sigma) = \frac{1}{2} \sigma^2 - \frac{1}{20} \sigma^4 + \frac{1}{6!} \sigma^6, \quad (29)$$

such that it is not convex in the UV. A plot of the UV potential can be found in Fig. 27 of Ref. [6]. This initial condition of the RG flow is chosen in Ref. [6] to test whether the poor convergence of the FRG Taylor expansion of the ϕ^4 -potential with negative mass term (28) is merely an artifact of the moving scale-dependent global minimum in the RG flow and to figure out whether the FRG Taylor expansion should have actually be performed at a moving expansion point, *i.e.*, about the moving global minimum instead of expanding around the IR minimum $\sigma = 0$ during the entire flow. However, although the global minimum at $\sigma = 0$ is not moving at all in the RG flow of the ϕ^6 -case (29), the Taylor expansion completely fails here,¹⁹ see Ref. [6]. In Ref. [6], we conclude that there has to be a time interval during the RG flow, where $u(t, x)$ exhibits a highly non-local dynamics. The latter cannot be captured by a local expansion with a finite number of couplings about a single point, even-though the expansion point is unique and does not move.

Actually, this can be seen directly from the RG flow of $u(t, x)$ in Fig. 7 at approximately $t \approx 27$, which is also the time when the RG flow of the Taylor-/vertex expansion collapses due to strongly oscillating and ultimately diverging couplings at $t \approx 27$. At this RG time, the local minimum (the second non-trivial zero-crossing) vaporizes via the diffusion and merges with the global minimum at $x = 0$. Already from the curves in Fig. 7 one can observe that the $u(t, x)$ is hardly describable over the entire RG flow with only a finite set of couplings. The breakdown of

¹⁷ At this point, one might be tempted to apply our definition of the normalized (numerical) entropy directly to some $\partial_x u(t, x)$ that is reconstructed from the flow of the coefficients of a Taylor expansion of the potential to study the validity of the expansion. However, this is not possible, because the FRG Taylor expansion in general provides only an adequate local description of the potential, while our (numerical) entropy or the TV requires knowledge about the global shape of the potential or its derivatives, respectively.

¹⁸ This reasoning might also resolve some issues, which are discussed in Ref. [33]. In Ref. [33], it is argued that the “ \mathcal{C} -theorem folklore” about the existence of a monotonically rising \mathcal{C} -function prevents the RG flow from entering limiting cycles (or even chaotic behavior) is wrong. However, their arguments are entirely based on examples of β -functions with a finite number of couplings. As explicitly shown in Ref. [33], such systems can indeed show limiting cycles and still have monotonic flows *etc.* as shown by the authors. Similar to what is explained at several occasions in our work, such systems do however not show irreversibility in the sense of a true diffusive/dissipative process or via the interaction/generation of discontinuities in field space – “the theory-space of couplings” [4, 7]. The only irreversible character of these systems might indeed be that they can enter limiting cycles, show chaotic behavior or enter fixed points on a finite set of couplings.

¹⁹ We thank J. Eser for discussions on this issue and a cross check which reproduced our findings for this test case, using his FRG code for Taylor-expanded effective actions [107, 135–137].

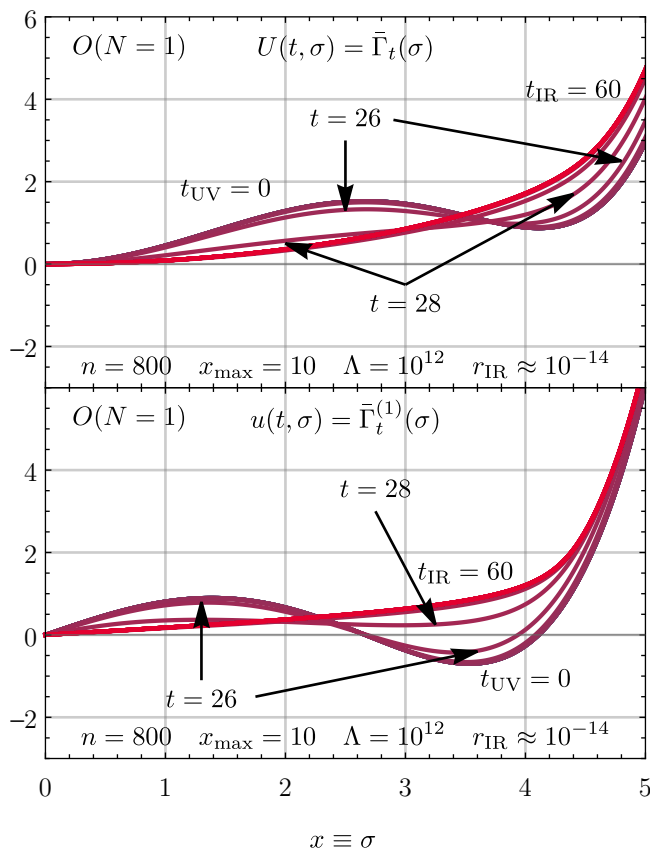


FIG. 7. RG flow of the effective potential $U(t, \sigma)$ (upper panel) and its derivative $u(t, \sigma) = \partial_\sigma U(t, \sigma)$ (lower panel) for the zero-dimensional $O(N = 1)$ -model with initial condition Eq. (29) evaluated at $t = 0, 2, 4, \dots, 60$ (integer values for t were only chosen for convenience and readability). The blue curve corresponds to the UV while the red curve to the IR. We used the exponential regulator Eq. (8) with UV cutoff $\Lambda = 10^6$. For convenience only, the plot does not show the region $x = 5$ to $x = 10$ because the tiny differences between $u(t, \sigma)$ and $u(t_{UV}, \sigma)$ are not visible in this region and vanish for large $x = \sigma$ anyhow.

any expansion can also be directly related to Wilbraham-Gibbs-oscillations [138–141] in the flat region of $u(t, x)$. This was already (indirectly) described before in the context of FRG studies [142] and represents another direct interplay between characteristic properties of the RG and the numeric treatment of PDEs.

Interestingly, also the (numerical) entropy function signals exactly the discussed non-local behavior at $t \approx 27$. Exactly at that point in time when the local minimum merges with the global minimum, we observe the strongest increase of entropy, see Fig. 8. We also find that by absolute measures, the entropy production for the ϕ^6 -initial potential (29) is greater than the entropy production observed for both quartic initial conditions (28). Nevertheless, the entropy production for the non-analytic initial condition (27) is still greater than the one in the ϕ^6 -case. This can be easily understood from the rela-

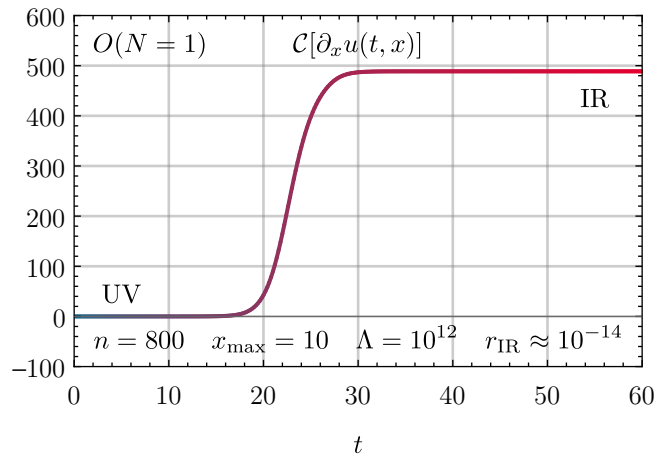


FIG. 8. The plot shows the monotonic growth of the (numerical) entropy/the \mathcal{C} -function $\mathcal{C}[\partial_x u(t, x)]$ during the RG flow of the test case (29) and corresponds to Fig. 7

tion of the numerical entropy to the total variation, *i.e.*, the arc length of $u(t, x)$ which even formally diverges for Eq. (27) in the UV.²⁰

We conclude from this section that the (numerical) entropy might be a tool to detect if the RG flow “moves” far from the perturbative region, while going from $t = 0$ to $t \rightarrow \infty$. In other words, it is a tool to discuss whether the RG flow is governed by strong (non-perturbative) dynamics and cannot be captured within any kind of local or perturbative expansion. This is analogous to a thermal system or fluid evolving through an out-of-equilibrium state, before finally equilibrating or showing steady flow behavior, in contrast to a temperature distribution or fluid that is already close to its equilibrium state.

D. Test case IV: the $\sigma = 0$ boundary

Our final test case has originally been used in part I of this series of publications [6] to test the correct implementation of (spatial) boundary conditions for PDEs of the form (10):

$$U(\sigma) = \begin{cases} -(\sigma^2)^{\frac{1}{3}}, & \text{if } |\sigma| \leq \sqrt{8}, \\ \frac{1}{2}\sigma^2 - 6, & \text{if } |\sigma| > \sqrt{8}. \end{cases} \quad (30)$$

The UV initial potential $U(\sigma)$ now exhibits a non-analyticity – a cusp – at $\sigma = 0$ which leads to a pole in the conserved quantity $u(t = 0, \sigma) = \partial_\sigma U(\sigma)$.²¹ Addi-

²⁰ Absolute values of the numerical entropy as well as their comparison should be considered with some care as explained above.

²¹ Potentials with cusps in field space can be found in the context of, *e.g.*, theories in 2+1 spacetime dimensions, such as the Gross-Neveu model [52].

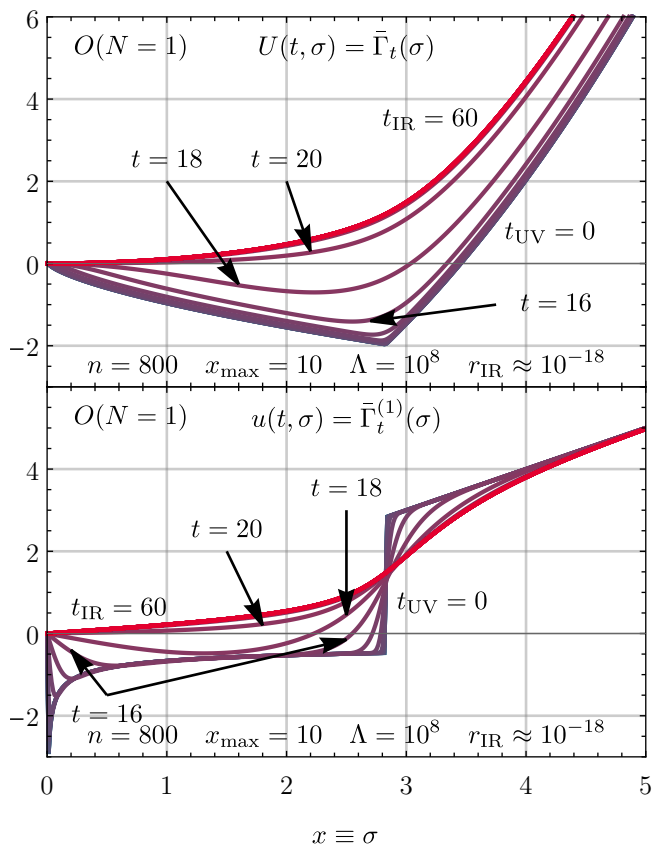


FIG. 9. The plot shows the RG flow of the effective potential $U(t, \sigma)$ (upper panel) and its derivative $u(t, \sigma) = \partial_\sigma U(t, \sigma)$ (lower panel) for the zero-dimensional $O(N = 1)$ -model with initial condition Eq. (30) evaluated at $t = 0, 2, 4, \dots, 60$ (integer values for t were only chosen for convenience and readability). The blue curve corresponds to the UV while the red curve to the IR. We used the exponential regulator Eq. (8) with UV cutoff $\Lambda = 10^6$. For convenience only, the plot does not show the region $x = 5$ to $x = 10$ because the tiny differences between $u(t, \sigma)$ and $u(t_{UV}, \sigma)$ are not visible in this region and vanish for large $x = \sigma$ anyhow.

tionally, to put the tests of our numerical approach to the extremes, we incorporated two non-trivial minima at $\sigma = \pm\sqrt{8}$, which are on top of that also non-analytic points, causing again discontinuities in $u(t = 0, \sigma)$. A visualization of Eq. (30) is shown in Fig. 30 of Ref. [6].

Also in the context of this work, the test case (30) turns out to be a highly interesting almost pathological example. The RG flow of $u(t, x)$ is shown in Fig. 9, where one can see that the numerical scheme indeed perfectly copes with the aforementioned somewhat artificial challenges and correctly reproduces symmetry restoration, convexity and smoothness of the potential in the IR regime.

Of specific interest regarding the (numeric) entropy is of course also the pole of $u(t = 0, x)$ at $x = 0$. Formally, the arc length (the total variation) of $u(t, x)$, which is directly related to our entropy function, diverges due to

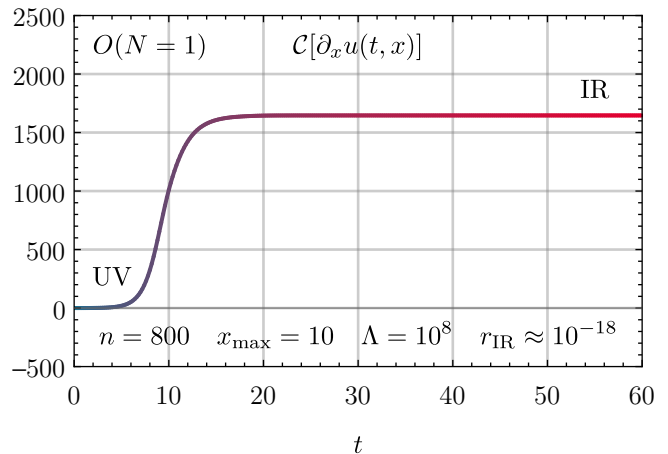


FIG. 10. The plot shows the monotonic growth of the (numerical) entropy/the \mathcal{C} -function $\mathcal{C}[\partial_x u(t, x)]$ during the RG flow of the test case (30) and corresponds to Fig. 9.

the pole at $t = 0$ for all $t > 0$. This divergence is of different nature than the divergence caused by integrating from $x = -\infty$ to $x = +\infty$ in Eq. (20). Whereas the latter can be cured by normalizing the entropy *w.r.t.* the entropy of $u(t = 0, x)$, the present divergence also occurs on the level of the “normalized” entropy function (21) similar to the other non-analytic jumps in the UV. The reason for the infinite entropy production while going from $t = 0$ to $t > 0$ is exactly that the total variation between $-x_{\max}$ and $+x_{\max}$ turns finite for $u(t, x)$ during the flow because the potential becomes convex and smooth. Moreover, symmetry restoration in the ground state sets in for $t \rightarrow \infty$. However, it is still normalized against the infinite total variation of $u(t = 0, x)$. Interestingly, this problem can be traced back to the initialization of the RG flow equations at $t = 0$ with the classical UV action $\bar{\Gamma}_{t=0}(\varphi) = \mathcal{S}(\varphi)$, which is actually not totally exact but rather an almost perfect approximation for sufficiently large Λ , see also our discussion in Ref. [6]. In Ref. [6], we argue that the extremely tiny errors stemming from this approximation of the correct initial condition are immediately “washed out” after the first RG steps (after an infinitesimal RG time step $\varepsilon > 0$) because of the diffusive character of the ERG equation (as long as Λ is chosen sufficiently large). This implies that we can safely ignore the problem of the infinite arc length at $t = 0$, and formally start considering the entropy from $t = \varepsilon$ onward.

From a purely practical and numerical perspective, these details may appear somewhat academic anyhow. Via the finite-volume discretization, a smallest resolution Δx in field space enters the problem which technically renders the pole at $\sigma = 0$ a huge but already finite jump captured in three volume cells on the level of the cell averages $\bar{u}_i(t)$ at $t = 0$. Therefore, we can use $u(t = 0, x)$ as our reference entropy for the normalization of Eq. (21) as it is numerically finite right from the beginning of the

flow.

An explicit result for the RG flow of our (numerical) entropy is shown in Fig. 10. Irrespective of the subtleties of the preceding discussion, we find a rather large entropy production at exactly those times when the pole vanishes and the jumps at $x = \pm\sqrt{8}$ are smeared out via the diffusion.

Additionally, we find that the total entropy production is much larger for this test case than for the previous ones. Again, this is of course directly related to the huge gradients in the initial condition, which are tremendous sources of entropy via dissipation, directly analogous to the heat equation.

In this section, we confronted our theoretical findings with direct numerical computations. We verified the behavior of the function $\mathcal{C}[\partial_x u(t, x)]$ from Eq. (21) by means of its discretized version in Eq. (24) as a valid numerical entropy in four test cases. Using the numerical entropy and the ERG equation in the form (10), we made several at this point almost intuitive connections between phenomena known in fluid and thermodynamic processes and directly related processes and aspects of RG flows. Most notable, the diffusive character of the flow equation (10) results directly in irreversible RG flows. This also establishes a connection between steady-state/(thermal) equilibrium solutions and the UV and IR regime. Moreover, the application of the numerical entropy and total variation appears to be an attractive monitor for RG consistency and the origin of an “thermodynamic” time asymmetry.

V. IRREVERSIBILITY OF THE RG FLOW, ENTROPY AND THE \mathcal{C} -THEOREM – GENERALIZATIONS

The (re-)discoveries within this work unravel the connection between the (numerical) entropy and total variation, employed in applied mathematics, and the irreversibility inherent to RG flows. Furthermore, they might even provide some connections to \mathcal{C} -/ \mathcal{A} -theorems within the framework of truncated RG flow equations. This section is dedicated to a discussion of these aspects of the RG and first generalizations of our findings from our zero-dimensional toy model to higher-dimensional theories.

A. The \mathcal{C} -theorem, fixed points and generalizations to (higher-dimensional) $O(N)$ models

The original formulation of the \mathcal{C} -theorem [26] states that for a two-dimensional field theory the following properties hold:

1. There exists a positive function

$$\mathcal{C}(\{g_i\}, t) \geq 0, \quad (31)$$

of all (possibly infinitely many) dimensionless couplings $\{g_i\}$ of the theory and RG time t , with the additional property

$$\frac{d}{dt} \mathcal{C}(\{g_i\}, t) \geq 0. \quad (32)$$

(The choice of sign is convention.)

2. The \mathcal{C} -function takes a fixed value at (critical) fixed points of the theory, these fixed values can be identified with the central charge c (of the Virasoro algebra)

$$\mathcal{C}(\{g_i^*\}, t) = c. \quad (33)$$

The central charge is different for different fixed points.

At first glance, it seems as if our numerical entropy (21) shares a lot of these properties because all (infinitely many) coupling constants are by definition dimensionless in $d = 0$ and all included via $u(t, x)$ in $\mathcal{C}[\partial_x u(t, x)]$. Furthermore, the function $\mathcal{C}[\partial_x u(t, x)]$ from Eq. (21) monotonically rises during the RG flow and clearly signals irreversibility – a central aspect of \mathcal{C} -/ \mathcal{A} -theorems [26–40]²². However, there is a crucial difference between our numerical entropy $\mathcal{C}[\partial_x u(t, x)]$ and the \mathcal{C} -function defined via Eqs. (31)–(33), which is more apparent if the discussion is generalized to higher dimensions.

As already briefly discussed, our previous results should also apply to higher-dimensional $O(1)$ models. This is directly understood by considering the LPA-flow equation of the d -dimensional $O(1)$ model using the LPA-optimized regulator [69, 70]. The corresponding flow equation for $u(t, x) = \partial_x U(t, x)$ then reads

$$\partial_t u(t, x) = \frac{d}{dx} \left(- \frac{A_d k^{d+2}(t)}{k^2(t) + \partial_\sigma u(t, \sigma)} \right), \quad (34)$$

where $A_d = \frac{\Omega_d}{d(2\pi)^d}$, and $\Omega_d = \frac{2\pi^{\frac{d}{2}}}{\Gamma(\frac{d}{2})}$ is the surface of the d -dimensional sphere and the definition (2) was used for the RG scale $k(t)$. Apart from numerical and k -dependent prefactors, which however do not affect the discussion for the numerical entropy in Sub.Sec. III A aside from the caveats already mentioned, the main differences between zero- and higher dimensions are:

1. In the zero-dimensional case, the PDE (10) represents a complete untruncated description of the QFT, while for higher-dimensional $O(1)$ models, the corresponding equation constitutes a truncation of the ERG equation (1). Still, on the level of

²² Generalizations of Zamolodchikov’s \mathcal{C} -theorem [26], especially from two to four dimensions, are often referred to as \mathcal{A} -theorems, referring to Ref. [29] in which an anomaly coefficient – hence \mathcal{A} -theorem – in four dimensions is proposed to take the role of the central charge which has given the original \mathcal{C} -theorem in two dimensions its name.

the PDE – thus within the LPA truncation – the definition of the numerical entropy function (21) can be used as an entropy and a detector for irreversibility. Additionally, it is not expected that a generic rise of the entropy during the RG flow gets lost, if more sophisticated truncations (like the inclusion of field-dependent wave function renormalizations) are studied because already the ERG equation (1) itself has the form of a non-linear diffusion equation. The numerical entropy (21) might even help to construct suitable truncation schemes as well as stable numerical methods.

2. In contrast to the zero-dimensional model, the couplings have in general non-zero energy dimensions. Thus, our numerical entropy (21) cannot adequately describe the second property of the \mathcal{C} -theorem (33) – namely capturing the properties of fixed points, which are defined via the zeroes of the β -functions of all dimensionless couplings and additionally a constant \mathcal{C} -/ \mathcal{A} -function. To capture the fixed-point structure, one has to replace (34) by its rescaled version and derive a corresponding numerical entropy functional.

Applying the transformations

$$y = A_d^{\frac{1}{2}} k^{-\frac{d-2}{2}}(t) x, \quad (35)$$

$$v(t, y) = A_d^{\frac{1}{2}} k^{-d}(t) u(t, x) \quad (36)$$

to Eq. (34), one arrives at the rescaled dimensionless RG flow equation for the derivative of the scale dependent effective potential,

$$\begin{aligned} \partial_t v(t, y) + \frac{d}{dy} F[y, v(t, y)] &= \quad (37) \\ &= \frac{d}{dy} Q[\partial_y v(t, y)] + S[v(t, y)], \end{aligned}$$

where

$$F[y, v(t, y)] \equiv \frac{d-2}{2} y v(t, y), \quad (38)$$

$$Q[\partial_y v(t, y)] \equiv -\frac{1}{1 + \partial_y v(t, y)}, \quad (39)$$

$$S[v(t, y)] \equiv d v(t, y). \quad (40)$$

Note that also in its rescaled dimensionless version, the flow equation (37) for the d -dimensional $O(1)$ model has the structure of a non-linear advection-diffusion-source/sink equation, similar to related RG flow equations in Refs. [14–18], where definition (38) corresponds to a position-dependent advection flux,²³

²³ For the $O(N)$ model with $N > 1$ the advection flux gains an additional contribution $-(N-1)/(1+v/y)$.

definition (39) corresponds to a non-linear diffusion flux, and, finally, definition (40) corresponds to a source/sink term. We can therefore completely stick to our fluid-dynamic interpretation in terms of conservation laws. Most notably, the diffusive character of the flow equation, thus irreversibility, is also manifest in its rescaled form, independent of the spacetime dimension d , see also Refs. [14–18] for related RG flow equations.

Using Eq. (37), the fixed-point solutions are defined as solutions of the equation with $\partial_t v(t, x) = 0$ because all other terms of the flow equation do not explicitly depend on t anymore. A corresponding (numerical) entropy function for Eq. (37), analogously to Eq. (21) should therefore signal irreversibility, associated with the change of the number of degrees of freedom for increasing RG time. In particular, it should also assume fixed values at fixed points of the RG flow. We would therefore expect a direct relation between (numerical) entropy in RG flows and Zamolodchikov’s formulation [26] or more recent [37, 38] formulations of the \mathcal{C} -function. In this respect, we note that it was possible to formulate \mathcal{C} -functions for the linearized version of the RG flow equation of the LPA [14–16, 27, 35].

Unfortunately, due to the explicitly position-dependent advection flux (37) as well as the source term (40), we were not able to formulate an appropriate numerical entropy measure yet.²⁴ When performing the y -derivative of the advection flux (38) in Eq. (37), thus considering the advection term in its primitive form, we can distinguish between a purely advective contribution $\propto \partial_y v(t, y)$ and an internal source term $\propto v(t, y)$. Source terms like $S[v(t, y)]$ from Eq. (40) and from position dependencies in non-linear advection or also diffusion fluxes make the construction of numerical entropy functions (like the TV) generally difficult. It is intuitively clear that source and sink terms can change and crucially increase the arc length – total variation – of solutions. The construction of numerical entropy functions and related numerical schemes for generic advection-diffusion-source/sink equations is still subject of ongoing research in numerical mathematics [143–146].

A promising next step might be studies of two-dimensional quantum field theories, where the advection

²⁴ The explicit position dependency of the advection flux also prevented us from formulating a numerical entropy for the zero-dimensional $O(N)$ model for finite $N > 1$. The corresponding contribution to the entropy function (21) allows for $\frac{d}{dt} \mathcal{C}[\partial_x u(t, x)] < 0$ during RG flow for certain initial conditions and N in the case of $N > 1$. For the zero-dimensional cases (28) and (29) discussed in this paper we find $\frac{d}{dt} \mathcal{C}[\partial_x u(t, x)] < 0$ during the RG evolutions for $N \geq 8$. For the cases (27) and (30) with their σ^2 asymptotics for large σ the inequality $\frac{d}{dt} \mathcal{C}[\partial_x u(t, x)] \geq 0$ seems to hold for all N and t . We further strongly believe that there are also counterexamples for higher-dimensional $O(N)$ models. Nevertheless, our numerical entropy function (21) for $N = 1$ might be a good starting point for generalizations to finite $N > 1$, other models and other truncations.

flux (38) vanishes for the $O(1)$ model also for the rescaled flow equation (37). For this case, the system entirely lacks advective contributions and the fields are not rescaled with k . Especially the last property might be interesting *w.r.t.* the spatial integration contained in the total variation (25), which consequently is k -independent for both – the dimensionful and dimensionless – formulations of the RG flow equation. Furthermore, for $d = 2$ one operates closest to the original version of Zamolodchikov’s \mathcal{C} -theorem [26], which should provide some additional guidance to relate the \mathcal{C} -theorem to numeric aspects of the PDEs that describe the RG flows.

Source terms arising from position-dependend advection- (in a formulation in x) and diffusion-terms (in a formulation in the invariant $\frac{1}{2}x^2$) when considering the PDEs in primitive form prevent an obvious generalization of the presented results to zero-dimensional $O(N)$ models with a finite amount $N > 1$ of scalars. In App. E 2 b of part III of this series of publications [7] we discuss numerical entropy and especially total variation/arc length as a candidate for the flow equations of the zero-dimensional $O(N)$ model at finite and notably infinite N . Reformulating the RG flow equation in the rescaled invariant $\frac{1}{2N}\sigma^2$ leads to a pure advection equation (with a non-linear but crucially position-independent flux) which are known to be TVNI [19, 55, 124], thus we identify the difference between initial and current TV as a numerical entropy functional in Eq. (E18) of Ref. [7].

Formulating a numerical entropy for the flow equation of the zero-dimensional $O(N)$ model at finite $N > 1$ might be an important first step towards a formulation in higher dimensions, since it would involve a treatment of source terms $\propto u(t, x)$. In this sense such a study would be similar to the study in two dimensions proposed in the previous paragraph. Here, a possible starting point might be the observations by Refs. [85, 86] that the zero-dimensional analogues of Dyson-Schwinger equations for the $O(N)$ model can be recast into a Virasoro algebra. The Virasoro algebra plays a central role in Zamolodchikov derivation of the \mathcal{C} -function for two-dimensional conformal field theories [26], while the Dyson-Schwinger equations are in direct relation to the RG equations. Also notable in this context is the fact that the Virasoro algebra arising in the study of zero-dimensional $O(N)$ model appears with vanishing central charge – in this limit strictly speaking as a Witt algebra – which considering Zamolodchikov definition of a \mathcal{C} -function indicates the absence of fixed points in RG flows of the zero-dimensional $O(N)$ model. This will be discussed elsewhere.

B. Pointwise monotonicity

Interestingly, the discussion of the previous paragraphs shows many similarities with the findings of Refs. [39, 40]. References [39, 40] discuss that for purely bosonic

models, the effective average action itself is a “pointwise monotonic function”, which can be directly seen from the signs of the bosonic contributions in the flow equation (1)²⁵. This implies

$$\partial_t \bar{\Gamma}_k[\Phi] \geq 0, \quad \forall \Phi. \quad (41)$$

However, Refs. [39, 40] argue that $\bar{\Gamma}_k[\Phi]$ cannot be directly used as a \mathcal{C} -function because – similar to our numerical entropy (21) – the above statement is only true for dimensionful field arguments and dimensionful couplings. However, as stated in [39, p. 3], “the \mathcal{C} -theorem and its generalizations apply to the RG flow on *theory space*, \mathcal{T} , a manifold which is coordinatized by the *dimensionless* couplings. The latter differ from the dimensionful ones by explicit powers of k fixed by the canonical scaling dimensions. As a consequence, when rewritten in terms of dimensionless fields and couplings, the property [(41)] does not precisely translate into a monotonicity statement about the de-dimensionalized theory space analog of $[\bar{\Gamma}_k]$, henceforth denoted \mathcal{A}_k . Rather, when the derivative ∂_k hits the explicit powers of k , additional canonical scaling terms arise which prevent us from concluding simply ‘by inspection’ that \mathcal{A}_k is monotonic along RG trajectories.”

In fact, we run into the same problems as Refs. [39, 40]. It is the trivial rescaling of dimensionful couplings in terms of the source term (40) that prevents us from immediately writing down an entropy functional or adapted total variation for our flow equation (37) (at least for $d = 2$) which could then be directly interpreted as a \mathcal{C} -function. In Refs. [39, 40], it is also the term related to the trivial rescaling which spoils the “pointwise monotonicity”.

VI. CONCLUSION AND OUTLOOK

In this article, we discussed several generic aspects of (F)RG flow equations. We based the discussion of our main findings on the rudimentary example of a zero-dimensional scalar QFT with \mathbb{Z}_2 -symmetry.

We started off by repeating and deepening the discussion of similarities between RG flow equations and (numerical) fluid dynamics, which was already started in part I of our series of publications [6]. Based on the formulation of RG flows as advection and diffusion driven dissipative flows in the field space of the corresponding QFT along RG scale (time), we argued that RG flows “produce” entropy. The RG scale (time) defines a rather natural “thermodynamic” arrow of time in this respect. We concluded that this dissipative character of the RG,

²⁵ Related statements about the general monotonicity of solutions of broad classes of PDEs/conservations laws are directly linked to the TVNI property, see *e.g.* Refs. [21, 24, 55] and especially Ref. [124].

which causes irreversibility of RG flows, is hard coded in the ERG equation (1). This implies that the irreversibility of Kadanoff’s block-spin picture is directly encoded in the PDEs (the field dependent β -functions), which describe the RG flows. Hereby, the IR solutions of RG flows represent equilibrium solutions of fluid dynamic equations. The impossibility of an unambiguous resolution of the microphysics (UV) from the macrophysics (IR) becomes apparent from this standpoint.

Furthermore, we explicitly demonstrated that the entropy production and the irreversibility during the RG flow from the UV to the IR are not only of abstract manner, but can – at least for flow equations in certain truncations – be quantified. Thereby, we directly related the entropy production to the numerical entropy production from the research field of PDEs and numerical fluid dynamics as well as to the total variation non-increasing property. The latter is used to ensure stability of numerical schemes for broad classes of PDEs.

Using our zero-dimensional toy model, we explicitly demonstrated for various test cases taken from our parallel publication [6] how numerical entropy is produced by diffusion in RG flows and non-analyticities in the UV-initial conditions.

Furthermore, we related certain aspects of the (numeric) entropy production in RG flows to the concept of \mathcal{C} -/ \mathcal{A} -theorems in RG theory since both manifestly encode the irreversible character of RG flows. However, our present study is not yet conclusive in this respect.

Although certain aspects of our discussion are still on an abstract level and could not yet be formalized in terms of explicit equations, we believe that our present work provides a fresh view on certain aspects of RG theory, embellished with at least a few new insights. In particular, our approach may help in the future to construct approximation schemes for RG studies which fully preserve the fundamentally dissipative character of RG flows.

ACKNOWLEDGMENTS

A.K., M.J.S., and J.B. acknowledge the support of the *Deutsche Forschungsgemeinschaft* (DFG, German Re-

search Foundation) through the collaborative research center trans-regio CRC-TR 211 “Strong-interaction matter under extreme conditions” – project number 315477589 – TRR 211.

A.K. acknowledges the support of the *Friedrich-Naumann-Foundation for Freedom*.

A.K. and M.J.S. acknowledge the support of the *Giersch Foundation* and the *Helmholtz Graduate School for Hadron and Ion Research*.

J.B. acknowledges support by the DFG under Grant No. BR 4005/4-1 and BR 4005/6-1 (Heisenberg program).

E.G. is supported by the U.S. Department of Energy, Office of Science, Office of Nuclear Physics, grants Nos. DE-FG-02-08ER41450.

N.W. is supported by the *Deutsche Forschungsgemeinschaft* (DFG, German Research Foundation) under Germany’s Excellence Strategy EXC 2181/1 - 390900948 (the Heidelberg STRUCTURES Excellence Cluster), the Collaborative Research Centre SFB 1225 (ISOQUANT), the BMBF grant 05P18VHFCA and from the Hessian collaborative research cluster ELEMENTS.

We thank the co-authors of the first part of this series of publications [6], M. Buballa and D. H. Rischke, for their collaboration, their support, and a lot of exceptionally valuable discussions.

We further thank F. Divotgey, J. Eser, F. Giacosa, F. Ihssen, L. Kurth, J. M. Pawłowski, K. Otto, R. D. Pisarski, S. Rechenberger, A. Sciarra, J. Stoll, and N. Zorbach for valuable discussions.

All numerical results as well as all figures in this work were obtained and designed using *Mathematica* [125] including the following *ResourceFunction*(s) from the *Wolfram Function Repository: PlotGrid* [147], *PolygonMarker* [148], and *MaTeXInstall* [149]. The “Feynman” diagram in Eq. (7) was generated with *Axodraw Version 2* [150].

-
- [1] L. P. Kadanoff, Scaling laws for Ising models near T_c , *Physics Physique Fizika* **2**, 263 (1966).
 - [2] K. G. Wilson, Problems in physics with many scales of length, *Sci. Am.* **241**, 140 (1979).
 - [3] N. Dupuis, L. Canet, A. Eichhorn, W. Metzner, J. M. Pawłowski, M. Tissier, and N. Wschebor, The non-perturbative functional renormalization group and its applications (2020), [arXiv:2006.04853](https://arxiv.org/abs/2006.04853) [[cond-mat.stat-mech](https://arxiv.org/abs/2006.04853)].
 - [4] E. Grossi and N. Wink, Resolving phase transitions with Discontinuous Galerkin methods (2019), [arXiv:1903.09503](https://arxiv.org/abs/1903.09503) [[hep-th](https://arxiv.org/abs/1903.09503)].
 - [5] E. Grossi, F. J. Ihssen, J. M. Pawłowski, and N. Wink, Shocks and quark-meson scatterings at large density (2021), [arXiv:2102.01602](https://arxiv.org/abs/2102.01602) [[hep-ph](https://arxiv.org/abs/2102.01602)].
 - [6] A. Koenigstein, M. J. Steil, N. Wink, E. Grossi, J. Braun, M. Buballa, and D. H. Rischke, Numerical fluid dynamics for FRG flow equations: Zero-dimensional QFTs as numerical test cases - Part I: The $O(N)$ model (2021), [arXiv:2108.02504](https://arxiv.org/abs/2108.02504) [[cond-mat.stat-mech](https://arxiv.org/abs/2108.02504)].
 - [7] M. J. Steil and A. Koenigstein, Numerical fluid dynamics for FRG flow equations: Zero-dimensional QFTs as numerical test cases - Part III: Shock and rarefaction

- waves in RG flows reveal limitations of the $N \rightarrow \infty$ limit in $O(N)$ -type models (2021), [arXiv:2108.04037 \[cond-mat.stat-mech\]](#).
- [8] N. Wink, *Towards the spectral properties and phase structure of QCD*, *Phd thesis*, University of Heidelberg (2020).
- [9] N. Wink, *Resolving phase transitions with Discontinuous Galerkin methods*, Talk at the EMMI Workshop Functional Methods in Strongly Correlated Systems (2019), [Online; accessed 2020.11.24].
- [10] M. J. Steil, A. Koenigstein, J. Braun, M. Buballa, E. Grossi, D. H. Rischke, and N. Wink, *Numerical fluid dynamics for FRG-flow equations: Zero-dimensional QFTs as numerical test cases*, Slides for the 10th International Conference on Exact Renormalization Group 2020 (ERG2020) (2020), [Online; accessed 2021.02.01].
- [11] J. Braun, M. Buballa, E. Grossi, A. Koenigstein, D. H. Rischke, M. J. Steil, and N. Wink, *Reanalysis of the phase diagram of the quark meson model in local potential approximation via the FRG*, in preparation (2021).
- [12] J. Stoll, N. Zorbach, A. Koenigstein, M. J. Steil, and S. Rechenberger, *Bosonic fluctuations in the (1 + 1)-dimensional Gross-Neveu(-Yukawa) model at varying μ and T and finite N* , in preparation (2021).
- [13] F. J. Ihssen, *Low-energy effective models of QCD at finite temperatures and densities*, master's thesis, University of Heidelberg (2020).
- [14] G. Zumbach, *Almost second order phase transitions*, *Phys. Rev. Lett.* **71**, 2421 (1993).
- [15] G. Zumbach, *The Local Potential Approximation of the Renormalization Group and its applications*, *Phys. Lett. A* **190**, 225 (1994).
- [16] G. Zumbach, *The Renormalization Group in the Local Potential Approximation and its applications to the $O(N)$ model*, *Nucl. Phys. B* **413**, 754 (1994).
- [17] A. Hasenfratz and P. Hasenfratz, *Renormalization Group study of scalar field theories*, *Nucl. Phys. B* **270**, 687 (1986).
- [18] G. Felder, *Renormalization group in the local potential approximation*, *Comm. Math. Phys.* **111**, 101 (1987).
- [19] P. D. Lax, *Hyperbolic Systems of Conservation Laws and the Mathematical Theory of Shock Waves*, in *Hyperbolic Systems of Conservation Laws and the Mathematical Theory of Shock Waves* (Society for Industrial and Applied Mathematics, 1973) pp. 1–48.
- [20] W. F. Ames, *Numerical Methods for Partial Differential Equations*, 3rd ed., Computer science and scientific computing (Academic Press, Boston [u.a.], 1992).
- [21] R. J. LeVeque, *Numerical methods for conservation laws*, 2nd ed. (Birkhäuser, Basel, 1992).
- [22] R. J. LeVeque, *Finite-volume methods for hyperbolic problems*, Cambridge Texts in Applied Mathematics (Cambridge University Press, 2002).
- [23] J. S. Hesthaven and T. Warburton, *Nodal Discontinuous Galerkin Methods: Algorithms, Analysis, and Applications*, 1st ed. (Springer Publishing Company, Incorporated, 2007).
- [24] E. F. Toro, *Riemann Solvers and Numerical Methods for Fluid Dynamics*, 3rd ed. (Springer-Verlag, Berlin, Germany, 2009).
- [25] L. Rezzolla and O. Zanotti, *Relativistic hydrodynamics* (Oxford University Press, Oxford, England, UK, 2018).
- [26] A. B. Zamolodchikov, *Irreversibility of the flux of the Renormalization Group in a 2D field theory*, *JETP Lett.* **43**, 730 (1986).
- [27] O. J. Rosten, *Fundamentals of the Exact Renormalization Group*, *Phys. Rept.* **511**, 177 (2012), [arXiv:1003.1366 \[hep-th\]](#).
- [28] T. Banks and E. J. Martinec, *The Renormalization Group and String Field Theory*, *Nucl. Phys. B* **294**, 733 (1987).
- [29] J. L. Cardy, *Is there a c -theorem in four dimensions?*, *Phys. Lett. B* **215**, 749 (1988).
- [30] H. Osborn, *Derivation of a four dimensional c -theorem for renormalisable quantum field theories*, *Phys. Lett. B* **222**, 97 (1989).
- [31] I. Jack and H. Osborn, *Analogues for the c -theorem for four-dimensional renormalizable field theories*, *Nucl. Phys. B* **343**, 647 (1990).
- [32] Z. Komargodski and A. Schwimmer, *On Renormalization Group flows in four dimensions*, *JHEP* **12**, 099, [arXiv:1107.3987 \[hep-th\]](#).
- [33] T. L. Curtright, X. Jin, and C. K. Zachos, *RG flows, cycles, and c -theorem folklore*, *Phys. Rev. Lett.* **108**, 131601 (2012), [arXiv:1111.2649 \[hep-th\]](#).
- [34] P. E. Haagensen, Y. Kubyshev, J. I. Latorre, and E. Moreno, *Gradient flows from an approximation to the Exact Renormalization Group*, *Phys. Lett. B* **323**, 330 (1994), [arXiv:hep-th/9310032](#).
- [35] J. Generowicz, C. Harvey-Fros, and T. R. Morris, *C function representation of the Local Potential Approximation*, *Phys. Lett. B* **407**, 27 (1997), [arXiv:hep-th/9705088](#).
- [36] S. Forte and J. I. Latorre, *A proof of the irreversibility of Renormalization Group flows in four-dimensions*, *Nucl. Phys. B* **535**, 709 (1998), [arXiv:hep-th/9805015](#).
- [37] A. Codello, G. D'Odorico, and C. Pagani, *A Functional RG equation for the c -function*, *JHEP* **07**, 040, [arXiv:1312.7097 \[hep-th\]](#).
- [38] A. Codello, G. D'Odorico, and C. Pagani, *Functional and local Renormalization Groups*, *Phys. Rev. D* **91**, 125016 (2015), [arXiv:1502.02439 \[hep-th\]](#).
- [39] D. Becker and M. Reuter, *Towards a C -function in 4D quantum gravity*, *JHEP* **03**, 065, [arXiv:1412.0468 \[hep-th\]](#).
- [40] D. Becker, *Asymptotically safe quantum gravity: Bimetric actions, boundary terms, & a C -function*, *Phd thesis*, Johannes Gutenberg University Mainz (2016).
- [41] J. L. Lebowitz, *Time's arrow and Boltzmann's entropy*, *Scholarpedia* **3**, 3448 (2008), revision #137152, [Online; accessed 2021.02.01].
- [42] C. Wetterich, *Exact evolution equation for the effective potential*, *Phys. Lett. B* **301**, 90 (1993), [arXiv:1710.05815 \[hep-th\]](#).
- [43] P. Deligne, P. I. Etingof, D. S. Freed, and A. M. Society, *Quantum fields and strings: a course for mathematicians*, Vol. 1 (American Mathematical Society Providence, 1999).
- [44] K. G. Wilson, *Renormalization group and critical phenomena. 1. Renormalization group and the Kadanoff scaling picture*, *Phys. Rev. B* **4**, 3174 (1971).
- [45] K. G. Wilson, *Renormalization group and critical phenomena. 2. Phase space cell analysis of critical behavior*, *Phys. Rev. B* **4**, 3184 (1971).
- [46] S. Weinberg, *Critical Phenomena for Field Theorists*, in *14th International School of Subnuclear Physics: Understanding the Fundamental Constituents of Matter* (1976).

- [47] S. Weinberg, What is quantum field theory, and what did we think it is?, in *Conference on Historical Examination and Philosophical Reflections on the Foundations of Quantum Field Theory* (1996) [arXiv:hep-th/9702027](#).
- [48] R. Percacci, Asymptotic Safety, in *Approaches to Quantum Gravity: Toward a New Understanding of Space, Time and Matter*, edited by D. Oriti (Cambridge University Press, Cambridge, 2007) Chap. 8, pp. 111–128, [arXiv:0709.3851 \[hep-th\]](#).
- [49] S. Weinberg, Living with Infinities (2009) [arXiv:0903.0568 \[hep-th\]](#).
- [50] M. Niedermaier and M. Reuter, The Asymptotic Safety Scenario in Quantum Gravity, *Living Rev. Rel.* **9**, 5 (2006).
- [51] A. Bonanno, A. Eichhorn, H. Gies, J. M. Pawłowski, R. Percacci, M. Reuter, F. Saueressig, and G. P. Vacca, Critical reflections on asymptotically safe gravity, *Front. in Phys.* **8**, 269 (2020), [arXiv:2004.06810 \[gr-qc\]](#).
- [52] J. Braun, H. Gies, and D. D. Scherer, Asymptotic safety: a simple example, *Phys. Rev. D* **83**, 085012 (2011), [arXiv:1011.1456 \[hep-th\]](#).
- [53] A. Jakovác, A. Patkós, and P. Pósfay, Non-Gaussian fixed points in fermionic field theories without auxiliary Bose-fields, *Eur. Phys. J. C* **75**, 2 (2015), [arXiv:1406.3195 \[hep-th\]](#).
- [54] A. Kurganov and E. Tadmor, New High-Resolution Central Schemes for Nonlinear Conservation Laws and Convection–Diffusion Equations, *Journal of Computational Physics* **160**, 241 (2000).
- [55] A. Harten, High resolution schemes for hyperbolic conservation laws, *Journal of Computational Physics* **49**, 357 (1983).
- [56] J. M. Pawłowski, Aspects of the functional renormalisation group, *Annals Phys.* **322**, 2831 (2007), [arXiv:hep-th/0512261](#).
- [57] J. Berges, N. Tetradis, and C. Wetterich, Nonperturbative renormalization flow in quantum field theory and statistical physics, *Phys. Rept.* **363**, 223 (2002), [arXiv:hep-ph/0005122](#).
- [58] P. Kopietz, L. Bartosch, and F. Schütz, *Introduction to the Functional Renormalization Group*, Lecture Notes in Physics, Vol. 798 (Springer-Verlag Berlin Heidelberg, 2010).
- [59] H. Gies, Introduction to the Functional RG and applications to gauge theories, *Lect. Notes Phys.* **852**, 287 (2012), [arXiv:hep-ph/0611146](#).
- [60] J. M. Pawłowski, J. A. Bonnet, S. Rechenberger, M. Reichert, and N. Wink, The functional renormalization group - applications to gauge theories and gravity, unpublished lecture notes in preparation.
- [61] B. Delamotte, An introduction to the nonperturbative Renormalization Group, *Lect. Notes Phys.* **852**, 49 (2012), [arXiv:cond-mat/0702365](#).
- [62] U. Ellwanger, Flow equations for N point functions and bound states, *Z. Phys. C* **62**, 503 (1994), [arXiv:hep-ph/9308260](#).
- [63] T. R. Morris, The Exact Renormalization Group and approximate solutions, *Int. J. Mod. Phys. A* **9**, 2411 (1994), [arXiv:hep-ph/9308265](#).
- [64] C. Wetterich, The average action for scalar fields near phase transitions, *Z. Phys. C* **57**, 451 (1993).
- [65] M. Reuter and C. Wetterich, Effective average action for gauge theories and exact evolution equations, *Nucl. Phys. B* **417**, 181 (1994).
- [66] M. Reuter, Nonperturbative evolution equation for quantum gravity, *Phys. Rev. D* **57**, 971 (1998), [arXiv:hep-th/9605030](#).
- [67] M. Reuter and F. Saueressig, Renormalization group flow of quantum gravity in the Einstein-Hilbert truncation, *Phys. Rev. D* **65**, 065016 (2002), [arXiv:hep-th/0110054](#).
- [68] J. Braun, H. Gies, and J. M. Pawłowski, Quark confinement from color confinement, *Phys. Lett. B* **684**, 262 (2010), [arXiv:0708.2413 \[hep-th\]](#).
- [69] D. F. Litim, Optimization of the exact renormalization group, *Phys. Lett. B* **486**, 92 (2000), [arXiv:hep-th/0005245](#).
- [70] J. M. Pawłowski, N. Strodthoff, and N. Wink, Finite temperature spectral functions in the $O(N)$ -model, *Phys. Rev. D* **98**, 074008 (2018), [arXiv:1711.07444 \[hep-th\]](#).
- [71] J. Braun, T. Dörfeld, B. Schallmo, and S. Töpfel, Renormalization Group studies of dense relativistic systems (2020), [arXiv:2008.05978 \[hep-ph\]](#).
- [72] H. Osborn and D. E. Twigg, Remarks on Exact RG equations, *Annals Phys.* **327**, 29 (2012), [arXiv:1108.5340 \[hep-th\]](#).
- [73] S. Weinberg, *The quantum theory of fields: Modern applications*, Vol. 2 (Cambridge University Press, Cambridge, England, UK, 1996).
- [74] M. E. Peskin and D. V. Schroeder, *An introduction to quantum field theory* (Addison-Wesley, Reading, USA, 1995).
- [75] J. Zinn-Justin, *Quantum field theory and critical phenomena*, 4th ed., Int. Ser. Monogr. Phys., Vol. 113 (Oxford University Press, 2002) pp. 1–1054, a Clarendon Press Publication.
- [76] J. Iliopoulos, C. Itzykson, and A. Martin, Functional methods and perturbation theory, *Rev. Mod. Phys.* **47**, 165 (1975).
- [77] B. S. DeWitt, *Dynamical theory of groups and fields* (Gordon and Breach, New York, USA, 1965).
- [78] W. Greiner and J. Reinhardt, *Field quantization* (Springer, Berlin Heidelberg, 1996).
- [79] A. Wipf, *Statistical approach to quantum field theory: An introduction*, Vol. 864 (Springer, Berlin, Heidelberg, 2013).
- [80] J. Polchinski, Renormalization and Effective Lagrangians, *Nucl. Phys. B* **231**, 269 (1984).
- [81] F. J. Wegner and A. Houghton, Renormalization Group equation for critical phenomena, *Phys. Rev. A* **8**, 401 (1973).
- [82] D. C. Brydges and T. Kennedy, Mayer expansions and the Hamilton-Jacobi equation, *J. Stat. Phys.* **48**, 19 (1987).
- [83] S. Hikami and E. Brezin, Large order behavior of the $1/N$ expansion in zero and one dimensions, *J. Phys. A* **12**, 759 (1979).
- [84] D. Bessis, C. Itzykson, and J.-B. Zuber, Quantum field theory techniques in graphical enumeration, *Adv. Appl. Math.* **1**, 109 (1980).
- [85] P. Di Vecchia, M. Kato, and N. Ohta, Double scaling limit in $O(N)$ vector models, *Nucl. Phys. B* **357**, 495 (1991).
- [86] S. Nishigaki and T. Yoneya, A nonperturbative theory of randomly branching chains, *Nucl. Phys. B* **348**, 787 (1991).
- [87] S. Schelstraete and H. Vershelde, Large N limit of

- $O(N)$ vector models, *Phys. Lett. B* **332**, 36 (1994), [arXiv:hep-th/9405158](#).
- [88] J. Zinn-Justin, Vector models in the large N limit: A Few applications, in *11th Taiwan Spring School on Particles and Fields* (1998) [arXiv:hep-th/9810198](#).
- [89] S. Flörchinger, Functional Renormalization and Ultracold Quantum Gases, Springer Theses [10.1007/978-3-642-14113-3](#) (2010).
- [90] S. Moroz, *Few-body physics with functional renormalization*, *Phd thesis*, University of Heidelberg (2011).
- [91] J. Keitel and L. Bartosch, The zero-dimensional $O(N)$ vector model as a benchmark for perturbation theory, the large- N expansion and the Functional Renormalization Group, *J. Phys. A* **45**, 105401 (2012), [arXiv:1109.3013 \[cond-mat.stat-mech\]](#).
- [92] F. Strocchi, *An introduction to non-perturbative foundations of quantum field theory*, Vol. 158 (Oxford University Press, Oxford, 2013).
- [93] S. Kemler and J. Braun, Towards a Renormalization Group approach to density functional theory – general formalism and case studies, *J. Phys. G* **40**, 085105 (2013), [arXiv:1304.1161 \[nucl-th\]](#).
- [94] J. M. Pawłowski, *Solving integrals with flow equations*, Slides for the lecture *Non-perturbative aspects of gauge theories* winter term 2012/2013 (2013), [Online; accessed 2020.10.29].
- [95] J. F. Rentrop, S. G. Jakobs, and V. Meden, Two-particle irreducible Functional Renormalization Group schemes – a comparative study, *Journal of Physics A: Mathematical and Theoretical* **48**, 145002 (2015).
- [96] D. S. Rosa, R. L. S. Farias, and R. O. Ramos, Reliability of the optimized perturbation theory in the 0-dimensional $O(N)$ scalar field model, *Physica A* **464**, 11 (2016), [arXiv:1604.00537 \[hep-ph\]](#).
- [97] H. Liang, Y. Niu, and T. Hatsuda, Functional Renormalization Group and Kohn-Sham scheme in density functional theory, *Phys. Lett. B* **779**, 436 (2018), [arXiv:1710.00650 \[cond-mat.str-el\]](#).
- [98] D. Skinner, *Lecture notes: Quantum Field Theory II* (2018), [Online; accessed 2021.01.12].
- [99] P. Millington and P. M. Saffin, Visualising quantum effective action calculations in zero dimensions, *J. Phys. A* **52**, 405401 (2019), [arXiv:1905.09674 \[hep-th\]](#).
- [100] E. Alexander, P. Millington, J. Nursey, and P. M. Saffin, Alternative flow equation for the Functional Renormalization Group, *Phys. Rev. D* **100**, 101702 (2019), [arXiv:1907.06503 \[hep-th\]](#).
- [101] A. G. Catalano, *Application of renormalization group techniques to the solution of integrals and Schrödinger eigenvalue equations*, *master's thesis*, Politecnico di Torino (2019).
- [102] P. Millington, *An alternative flow equation from the regulator-sourced 2PI effective action*, Talk at the 10th International Conference on Exact Renormalization Group 2020 (ERG2020) (2020), [Online; accessed 2021.01.12].
- [103] P. Millington and P. M. Saffin, Benchmarking regulator-sourced 2PI and average 1PI flow equations in zero dimensions (2021), [arXiv:2107.12914 \[hep-th\]](#).
- [104] L. Kades, M. Gärttner, T. Gasenzer, and J. M. Pawłowski, Towards sampling complex actions (2021), [arXiv:2106.09367 \[hep-lat\]](#).
- [105] B.-J. Schaefer, O. Bohr, and J. Wambach, Finite temperature gluon condensate with renormalization group flow equations, *Phys. Rev. D* **65**, 105008 (2002), [arXiv:hep-th/0112087](#).
- [106] J. Braun, M. Leonhardt, and J. M. Pawłowski, Renormalization group consistency and low-energy effective theories, *SciPost Phys.* **6**, 056 (2019), [arXiv:1806.04432 \[hep-ph\]](#).
- [107] N. Cichutek, F. Divotgey, and J. Eser, Fluctuation-induced higher-derivative couplings and infrared dynamics of the quark-meson-diquark model, *Phys. Rev. D* **102**, 034030 (2020), [arXiv:2006.12473 \[hep-ph\]](#).
- [108] N. D. Mermin and H. Wagner, Absence of ferromagnetism or antiferromagnetism in one- or two-dimensional isotropic Heisenberg models, *Phys. Rev. Lett.* **17**, 1133 (1966).
- [109] P. C. Hohenberg, Existence of long-range order in one and two dimensions, *Phys. Rev.* **158**, 383 (1967).
- [110] S. R. Coleman, There are no Goldstone bosons in two-dimensions, *Commun. Math. Phys.* **31**, 259 (1973).
- [111] M. Salmhofer, *Rigorous Renormalization Group*, Talk at the 10th International Conference on Exact Renormalization Group 2020 (ERG2020) (2020), [Online; accessed 2021.01.12].
- [112] K.-I. Aoki, S.-I. Kumamoto, and M. Yamada, Phase structure of the NJL model with weak renormalization group, *Nucl. Phys. B* **931**, 105 (2018), [arXiv:1705.03273 \[hep-th\]](#).
- [113] W. J. M. Rankine, On the thermodynamic theory of waves of finite longitudinal disturbance, *Phil. Trans. R. Soc.* **160**, 277 (1870).
- [114] P.-H. Hugoniot, On the propagation of motion in bodies and in perfect gases in particular – I, in *Classic papers in shock compression science*, edited by J. N. Johnson and R. Chéret (Springer, New York, 1998) pp. 161–243, translation of: Hugoniot, Pierre-Henri, *Journal de l'École Polytechnique*, Vol. **57**, pp. 3 – 97 (1887).
- [115] N. Tetradis and D. F. Litim, Analytical solutions of exact renormalization group equations, *Nucl. Phys. B* **464**, 492 (1996), [arXiv:hep-th/9512073](#).
- [116] K.-I. Aoki, S.-I. Kumamoto, and D. Sato, Weak solution of the non-perturbative renormalization group equation to describe dynamical chiral symmetry breaking, *PTEP* **2014**, 043B05 (2014), [arXiv:1403.0174 \[hep-th\]](#).
- [117] H. Bateman, Some recent researches on the motion of fluids, *Monthly Weather Review* **43**, 163 (1915).
- [118] J. M. Burgers, A mathematical model illustrating the theory of turbulence, *Advances in Applied Mechanics* **1**, 171 (1948).
- [119] J. R. Cannon, *The one-dimensional heat equation* (Cambridge University Press, 1984).
- [120] V. Pangon, S. Nagy, J. Polonyi, and K. G. Sailer, Onset of symmetry breaking by the Functional RG method, *Int. J. Mod. Phys. A* **26**, 1327 (2011), [arXiv:0907.0144 \[hep-th\]](#).
- [121] J. Borchardt and B. Knorr, Global solutions of functional fixed point equations via pseudospectral methods, *Phys. Rev. D* **91**, 105011 (2015), [Erratum: *Phys. Rev. D* **93**, 089904 (2016)], [arXiv:1502.07511 \[hep-th\]](#).
- [122] J.-M. Caillol, The non-perturbative renormalization group in the ordered phase, *Nucl. Phys. B* **855**, 854 (2012), [arXiv:1109.4024 \[cond-mat.stat-mech\]](#).
- [123] J. Borchardt and B. Knorr, Solving functional flow equations with pseudo-spectral methods, *Phys. Rev. D* **94**, 025027 (2016), [arXiv:1603.06726 \[hep-th\]](#).
- [124] R. M. Redheffer and W. Walter, The total variation of

- solutions of parabolic differential equations and a maximum principle in unbounded domains, *Math. Ann.* **209**, 57 (1974).
- [125] Wolfram Research, Inc., *Mathematica, Version 12.1* (2020), Champaign, IL.
- [126] Y. Fujimoto, L. O’Raifeartaigh, and G. Parravicini, Effective potential for non-convex potentials, *Nucl. Phys. B* **212**, 268 (1983).
- [127] J. Zinn-Justin, Critical Phenomena: field theoretical approach, *Scholarpedia* **5**, 8346 (2010), revision #148508.
- [128] Y. Nambu, Quasiparticles and gauge invariance in the theory of superconductivity”, *Phys. Rev.* **117**, 648 (1960).
- [129] J. Goldstone, Field theories with superconductor solutions, *Nuovo Cim.* **19**, 154 (1961).
- [130] J. Goldstone, A. Salam, and S. Weinberg, Broken symmetries, *Phys. Rev.* **127**, 965 (1962).
- [131] H. D. Politzer, Reliable perturbative results for strong interactions?, *Phys. Rev. Lett.* **30**, 1346 (1973).
- [132] D. J. Gross and F. Wilczek, Ultraviolet behavior of non-Abelian gauge theories, *Phys. Rev. Lett.* **30**, 1343 (1973).
- [133] D. J. Gross and F. Wilczek, Asymptotically free gauge theories. I, *Phys. Rev. D* **8**, 3633 (1973).
- [134] D. J. Gross and F. Wilczek, Asymptotically free gauge theories. II, *Phys. Rev. D* **9**, 980 (1974).
- [135] J. Eser, F. Divotgey, M. Mitter, and D. H. Rischke, Low-energy limit of the $O(4)$ quark-meson model from the functional renormalization group approach, *Phys. Rev. D* **98**, 014024 (2018), arXiv:1804.01787 [hep-ph].
- [136] J. Eser, F. Divotgey, and M. Mitter, Low-energy limit of the $O(4)$ quark-meson model, *PoS CD2018*, 060 (2019), arXiv:1902.04804 [hep-ph].
- [137] F. Divotgey, J. Eser, and M. Mitter, Dynamical generation of low-energy couplings from quark-meson fluctuations, *Phys. Rev. D* **99**, 054023 (2019), arXiv:1901.02472 [hep-ph].
- [138] H. Wilbraham, On a certain periodic function, *Cambridge and Dublin Mathematical Journal* **3**, 198 (1848).
- [139] J. W. Gibbs, Fourier’s series, *Nature* **59**, 200 (1898).
- [140] J. W. Gibbs, Fourier’s series, *Nature* **59**, 606 (1899).
- [141] J. P. Boyd, *Chebyshev and Fourier spectral methods*, 2nd ed. (Dover Publications, Mineola, New York, 2001) 1st ed. in 1969 by Springer-Verlag, Berlin Heidelberg, in the series *Lecture Notes in Engineering, Vol. 49*.
- [142] V. Pangon, Structure of the broken phase of the sine-Gordon model using Functional Renormalization, *Int. J. Mod. Phys. A* **227**, 1250014 (2012), arXiv:1008.0281 [hep-th].
- [143] L. Monthé, A study of splitting scheme for hyperbolic conservation laws with source terms, *Journal of Computational and Applied Mathematics* **137**, 1 (2001).
- [144] R. D. Beneito and A. M. Gavara, A ‘TVD-like’ Scheme for Conservation Laws with Source Terms, in *Numerical Mathematics and Advanced Applications* (Springer, Berlin, Germany, 2008) pp. 265–272.
- [145] R. Chen and D.-k. Mao, Entropy-TVD Scheme for Nonlinear Scalar Conservation Laws, *J. Sci. Comput.* **47**, 150 (2011).
- [146] M. Bessemoulin-Chatard and F. Filbet, A Finite Volume Scheme for Nonlinear Degenerate Parabolic Equations, *SIAM Journal on Scientific Computing* **34**, B559–B583 (2012).
- [147] L. Lang, *Wolfram Mathematica function repository: ResourceFunction PlotGrid* (2020), [Online; accessed 2020.10.08].
- [148] A. Popkov, *Wolfram Mathematica function repository: ResourceFunction PolygonMarker* (2020), [Online; accessed 2020.10.08].
- [149] S. Horvát, *MaTeX* (2020), [Online; accessed 2020.10.08].
- [150] J. C. Collins and J. A. Vermaseren, Axodraw version 2 (2016), arXiv:1606.01177 [cs.OH].